

1 **Ensemble streamflow prediction considering the influence of  
2 reservoirs in Narmada River basin, India**

3

4 Urmin Vegad<sup>1</sup> and Vimal Mishra<sup>1,2\*</sup>

5

6 <sup>1</sup>Civil Engineering, Indian Institute of Technology (IIT) Gandhinagar

7 <sup>2</sup>Earth Sciences, Indian Institute of Technology (IIT) Gandhinagar

8 \*Corresponding author: [vmishra@iitgn.ac.in](mailto:vmishra@iitgn.ac.in)

9 **Abstract**

10 Developing an ensemble hydrological prediction system is essential for reservoir operations and flood early  
11 warning. However, efforts to build hydrological ensemble prediction systems considering the influence of  
12 reservoirs have been lacking in India. We examine the potential of the Extended Range Forecast System (ERFS,  
13 16 ensemble members) and Global Ensemble Forecast System (GEFS, 21 ensemble members) forecast for  
14 streamflow prediction in India using the Narmada River basin as a testbed. We use the Variable Infiltration  
15 Capacity (VIC) with reservoir operations (VIC-Res) scheme to simulate the daily river flow at four locations in  
16 the Narmada basin. Streamflow prediction skills of the ERFS forecast were examined for the period 2003-2018 at  
17 1-32 day lead. We compared the streamflow forecast skills of raw meteorological forecasts from ERFS and GEFS  
18 at a 1-10 day lead for the summer monsoon (June-September) 2019-2020. The ERFS forecast underestimates  
19 extreme precipitation against the observations compared to the GEFS forecast during the summer monsoon of  
20 2019-2020. However, both the forecast products show better skills for minimum and maximum temperatures than  
21 precipitation. Ensemble streamflow forecast from the GEFS performs better than the ERFS during 2019-2020.  
22 The performance of GEFS based ensemble streamflow forecast declines after five days lead. Overall, the GEFS  
23 ensemble streamflow forecast can provide reliable skills at a 1-5 day lead, which can be utilized in streamflow  
24 prediction. Our findings provide directions for developing a flood early warning system based on ensemble  
25 streamflow prediction considering the influence of reservoirs in India.

26 **1. Introduction**

27 Floods are one of India's most destructive and frequently occurring natural disasters. Floods accounted for about  
28 47% of natural disasters in India during the last 100 years (Tripathi, 2016). Riverine floods occur during the  
29 summer monsoon season affecting approximately five million people annually (Luo et al., 2015). Singh and Kumar  
30 (2013) reported an increase in the frequency of floods in India. About 20% of the total flood-prone area gets  
31 affected every year (Ray et al., 2019). Floods in 2018 caused an economic loss of more than twelve billion dollars

32 (USD) and resulted in the loss of 1808 lives (Joshi, 2020). In addition, climate warming is projected to increase  
33 the frequency and intensity of riverine floods (Field et al., 2011; Luo et al., 2015; Nanditha and Mishra, 2022; Ali  
34 et al., 2019).

35

36 Preparedness for disasters like floods can help in mitigating economic loss and reducing flood mortality (Jain et  
37 al., 2018). While losses due to floods are projected to rise under the warming climate, human mortality can be  
38 reduced with flood early warning systems and effective communication (Dipti, 2017, Nanditha and Mishra, 2021).  
39 Therefore, developing a robust flood prediction system is necessary for early warning and preparedness.  
40 Streamflow prediction is an essential component of flood forecasting, which helps in planning and decision-  
41 making (Georgakakos et al., 2012; Alfieri et al., 2013). Most of the streamflow prediction systems in India are  
42 based on the deterministic approach (Harsha, 2020a; Todini, 2017, Nanditha and Mishra, 2021), which do not  
43 account for perturbations in initial conditions to quantify the uncertainty (Bowler et al., 2008). Uncertainty  
44 quantification in streamflow prediction can reduce the risk of false alarms based on deterministic forecast (Todini,  
45 2017). In addition, ensemble streamflow prediction is essential for the probabilistic flood forecast. The  
46 probabilistic approach performs better than the deterministic approach by quantifying uncertainties associated with  
47 flood prediction and early warning system (Krzysztofowicz, 2001). Previous studies used ensemble streamflow  
48 prediction in flood forecasting (Cloke and Pappenberger, 2009; Wu et al., 2020) using ensemble meteorological  
49 forecast and hydrological models (Zhang et al., 2020). Ensemble weather forecast provides multiple members at  
50 the same location and time that can be used for probabilistic hydrological prediction. However, several challenges  
51 are associated with the operational ensemble streamflow forecast, including computational limitations, explanation  
52 of ensemble forecasts to non-experts, and up-gradation in the policy to use the forecast for decision making  
53 (Demeritt et al., 2010; Arnal et al., 2020). Despite these challenges, ensemble flood forecasts consider the  
54 uncertainty that can be used for preparedness and planning compared to the deterministic forecast approach.  
55 (Pappenberger et al., 2012; Cloke and Pappenberger, 2009).

56

57 Indian river basins are considerably affected by human interventions including presence of reservoirs, water  
58 withdrawal for irrigation, and inter/intra basin water transfer (Nanditha and Mishra, 2021; Madhusoodhanan et al.,  
59 2016; Gosain et al., 2006). India has more than 5000 large dams while about 450 are currently under construction  
60 (NRLD, 2017). Reservoirs and irrigation can considerably modulate terrestrial water and energy budgets in India  
61 (Shah et al., 2019). For instance, Shah et al. (2019) showed that evapotranspiration and latent heat flux are  
62 increased under the presence of irrigation and reservoirs in Indian river basins compared to their natural conditions.  
63 Dong et al. (2022) reported that reservoirs can significantly (~ 25%) contribute to the variation of terrestrial water  
64 storage in China. In addition, the presence of reservoirs can considerably affect streamflow variability in the  
65 downstream regions (Zajac et al., 2017; Yun et al., 2020; Chai et al., 2019). Reservoirs in India are multipurpose  
66 as these store water for the dry season, generate hydropower, and attenuate floods in the downstream regions  
67 (Tiwari and Mishra, 2022). Reservoirs store water during the summer monsoon season and release water during

68 the dry season for irrigation. Similarly, based on the reservoir rule curve, a buffer storage is kept during the wet  
69 season to accommodate high inflow so that flood risk can be minimized in the downstream region. Therefore,  
70 there are several challenges associated with the streamflow forecast in the river basins that are affected by  
71 reservoirs. Most often hydrological model-based flood/streamflow forecast does not consider the influence of  
72 reservoirs that could lead to under or overestimation of flow depending on the season (Nanditha and Mishra, 2021;  
73 Dang et al., 2019). Incorporating reservoir influence in hydrological models is essential as reservoirs significantly  
74 affect the magnitude and timing of streamflow (Zajac et al., 2017; Yassin et al., 2019; Dang et al., 2019). Several  
75 efforts have been made to incorporate the influence of reservoirs in the hydrological models (Boulange Julien and  
76 Hanasaki Naota, 2013; Dang et al., 2019; Hanasaki et al., 2018). However, most of the previous studies on flood  
77 forecasts and early warnings in India did not consider the influence of reservoirs (Goswami et al., 2018; Sikder  
78 and Hossain, 2019).

79

80 The Central Water Commission (CWC) manages flood forecast systems in India. The flood forecast network  
81 monitors 325 stations across India. CWC observes real-time water level and discharge along the major rivers of  
82 India during the designated flood period. The flood forecast is performed using statistical correlation methods  
83 from gauge to gauge. Moreover, Quantitative Precipitation Forecast (QPF) from the India Meteorological  
84 Department (IMD) is used to forecast floods at a 3-day lead time (Teja and Umamahesh, 2020). The current model-  
85 based flood forecast approach used by CWC is deterministic, which lacks incorporating uncertainties in the  
86 forecast and early warning system. An ensemble forecast system can help in flood early warning and decision-  
87 making (Harsha, 2020b; Nanditha and Mishra, 2021). Various ensemble forecast products are available from the  
88 India Meteorological Department (IMD) and the Indian Institute of Tropical Meteorology (IITM). However, the  
89 utility of these forecast products for streamflow prediction and flood early warning at the river basin scale has not  
90 been examined. In addition, despite the advantages of ensemble hydrological prediction, India's current  
91 hydrological forecast systems are mainly deterministic. Given the increasing flood damage in India, the  
92 overarching aim of this work is to explore the utility of ensemble forecast products for streamflow prediction in  
93 India. We considered the Narmada River basin as a testbed to examine the potential of ensemble hydrological  
94 prediction. We used the Variable Infiltration Capacity (VIC) with reservoir operations (VIC-Res) scheme, which  
95 incorporates the effect of reservoirs (Dang et al., 2019). Extended Range Forecast System (ERFS) and Global  
96 Ensemble Forecast System (GEFS) ensemble forecasts developed by IITM are used to examine the hydrological  
97 prediction skills at the selected gauge stations in the Narmada basin.

98

## 99 **2. Data and methods**

### 100 **2.1 Study region and datasets**

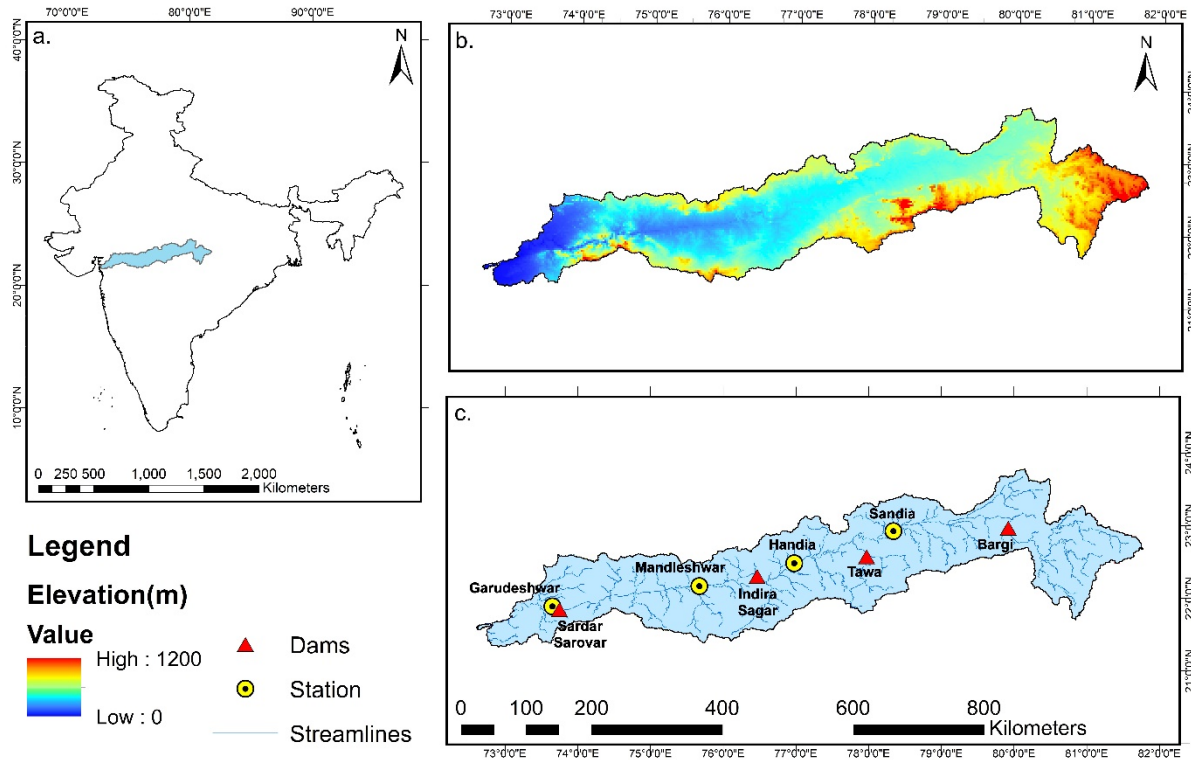
101 Narmada is the fifth biggest and the largest west-flowing river in India. The Narmada river basin falls in two states,  
102 Gujarat and Madhya Pradesh. Many tributaries contribute to the river through its way to the Arabian Sea, with the

103 Tawa river being its longest tributary. The catchment area of the river basin at the outlet is approximately 98,796  
104 km<sup>2</sup>. The upper portion of the basin falls in Madhya Pradesh. The mean annual rainfall in the Narmada basin is  
105 1064 mm. Most of the total annual precipitation occurs during the summer monsoon season (June-September).  
106 We used observed daily streamflow at four stations: Sandia, Handia, Mandleshwar, and Garudeshwar (Fig. 1).  
107 There are several ongoing hydropower and irrigation projects in the Narmada basin. Our hydrological modelling  
108 framework has considered four dams: Bargi, Tawa, Indira Sagar, and Sardar Sarovar (Table 1). Bargi and Tawa  
109 reservoirs were primarily constructed for irrigation purposes (Table 1). At the same time, Indira Sagar (0.975  
110 Billion Cubic Meters (BCM)) and Sardar Sarovar (5.8 BCM) are the two largest reservoirs that are used for multi-  
111 purpose.

112 **Table 1. Parameters of reservoirs that were considered in hydrological simulations**

Sr No	Name of dam	Year of completion	Height above lower foundation (m)	Length of dam (m)	Gross storage capacity (BCM)	Effective storage capacity (BCM)
1	Bargi	1988	69.8	5357	3.92	3.18
2	Tawa	1978	57.92	1944.92	2.312	1.94
3	Indira Sagar	2006	91.4	654	12.22	9.75
4	Sardar Sarovar	2017	163	1210	9.5	5.8

113



114

115 **Figure 1. Basic information about (a) location in India, (b) topography, c) streamlines, location of streamflow gauge**  
 116 **stations and reservoirs**

117 We used  $0.25^\circ$  (approximate spatial resolution;  $\sim 27.5 \times 27.5$  km) gridded daily precipitation from IMD for the  
 118 1951-2020 period (Pai et al., 2014). The daily gridded precipitation product is developed using observations from  
 119 6955 rain gauge stations (Pai et al., 2015). Pai et al. (2015) examined daily rainfall trends, long-term climatology,  
 120 and variability over the central Indian region. The high resolution ( $0.25^\circ$ ) gridded precipitation captures spatial  
 121 variability in better manner compared to previous coarse-gridded rainfall products. We obtained daily  $1^\circ$  gridded  
 122 maximum and minimum temperatures from IMD (Srivastava et al., 2009). Srivastava et al. (2009) developed the  
 123 gridded temperature dataset using observations from 395 stations. We used bilinear interpolation to convert the  $1^\circ$   
 124 gridded temperature to  $0.25^\circ$  resolution to make it consistent with the gridded precipitation. The VIC model also  
 125 requires daily wind speed as an input. We obtained the wind speed from the National Centers for Environmental  
 126 Prediction (NCEP)-National Centers for Atmospheric Research (NCAR)  
 127 (<https://psl.noaa.gov/data/gridded/data.ncep.reanalysis.pressure.html>). The wind speed at a coarser ( $1.875^\circ \times$   
 128  $1.905^\circ$ ) resolution was interpolated using bilinear interpolation to  $0.25^\circ$  to make it consistent with the other  
 129 meteorological datasets. The VIC model's vegetation parameters were obtained from the Advanced Very High-  
 130 Resolution Radiometer (AVHRR) global land cover, which is available at 1-km spatial resolution (Sheffield and  
 131 Wood, 2007). Soil parameters at  $0.25^\circ$  were developed using the Harmonized World Soil Database (HWSD  
 132 version 1.2) [Gao et al., 2009]. We used digital elevation model data from Shuttle Radar Topography Mission

133 (SRTM) at 90 m spatial resolution (Jarvis, 2008). The hydrological model considers sub-grid variability of  
134 topography and vegetation (Gao et al. 2010). Therefore, the high-resolution vegetation and elevation datasets were  
135 used to extract values for different tiles within a grid.

136 We obtained observed daily streamflow, reservoir water level, and reservoir live storage data from the India -  
137 Water Resources Information System (IWRIS; <http://www.indiawris.gov.in>), which is a joint venture of the  
138 Central Water Commission, the Ministry of Jal Shakti, and the Indian Space Research Organization (ISRO).  
139 Streamflow and reservoir levels are monitored at various locations in the Narmada basin by CWC. We selected  
140 the gauge stations (Sandia, Handia, Mandleshwar, and Garudeshwar) that have observed flow data for at least 15  
141 years. The reservoir storage and water level data were obtained for different periods depending on the data  
142 availability.

143 We obtained the Extended Range Forecast System (ERFS) meteorological forecast for the 2003-2020 period. In  
144 addition, the Global Ensemble Forecast System (GEFS) meteorological forecast was obtained for the summer  
145 monsoon season (July-September) of 2019-2020 from the IITM. Both the ERFS and GEFS forecast products are  
146 developed at IITM and are currently being used for the operational weather forecast by the IMD. In June 2018,  
147 the high-resolution GEFS forecast was developed and then transferred to the IMD for operational forecasting  
148 (Mukhopadhyay et al., 2018). The GEFS dataset has a horizontal resolution of T1534 (~12.5 km) and consists of  
149 21 ensemble members (one control and twenty perturbed). The dynamic core of the model is based on semi-  
150 Lagrangian framework, which reduces considerable computational requirements. The initial conditions (ICs) for  
151 meteorological forecasts are obtained from Global Data Assimilation System (GDAS). The GEFS is being run  
152 operationally for the ten-day lead forecast using daily Initial Conditions (ICs) during the summer monsoon period.  
153 The GEFS forecast successfully predicted the 2018 Kerala extreme rainfall at 2-3 days lead and showed reasonable  
154 forecast skills at 5-7 days lead (Mukhopadhyay et al., 2018).

155 The ERFS multi-model system consists of four (CFSv2T382, CFSv2T126, GFSbcT382 and GFSbcT126) suites,  
156 each having four ensemble members (one control and three perturbed). Therefore, sixteen ensemble members are  
157 available for the ERFS forecast. The model is being run operationally for 32 days lead based on the initial  
158 conditions of every Wednesday. Atmospheric and oceanic initial conditions from the National Center for Medium-  
159 Range Weather Forecasting (NCMWRF) and Indian National Centre for Ocean Information Services (INCOSIS)  
160 assimilation system are used by the models in ERFS. We used the sixteen ensemble meteorological forecasts to  
161 simulate the daily streamflow at 1-32 days leads at selected stations in the Narmada river basin. Shah et al. (2017)  
162 reported that ERFS performed better than the Global Ensemble Forecast System v2 (GEFSv2) and Climate  
163 Forecast System v2 (CFSv2) in precipitation forecast during the summer monsoon season over India.

164 **2.2 The VIC-Res hydrological model**

165 We used the VIC-Res hydrological model (Dang et al., 2019), a novel variant of the VIC model (Liang et al.,  
166 1994), to simulate streamflow. A combination of the VIC model and the routing model developed by Dang et al.  
167 (2019) was used to simulate streamflow at the selected locations in the basin. Dang et al. (2019) incorporated the  
168 effect of reservoirs by considering the reservoir storage dynamics and operating rules within the streamflow  
169 routing model in the VIC-Res model. The rainfall-runoff model generates water and energy fluxes within each  
170 grid using climate forcing, soil parameters, land use/land cover, and the digital elevation model. The model uses  
171 vegetation cover for each tile and three soil layers for each grid cell. The upper two soil layers control runoff,  
172 infiltration, and evaporation, while the bottom layer governs baseflow. The routing model uses water fluxes (runoff  
173 and baseflow) from each grid to simulate streamflow at selected gauge stations using the linearized Saint-Venant  
174 equations. The routing model uses flow direction, fractional area within a grid, and station location as input to  
175 generate streamflow. In addition, the VIC-Res model requires reservoir parameters and location as inputs. The  
176 reservoir parameters include full reservoir level (FRL), dead water level, storage capacity, dead storage, rated  
177 head, and the year when reservoir became operational. The VIC-Res considers a grid as a reservoir and the  
178 incoming streamflow to that reservoir is considered as the inflow. In addition to the reservoir parameters, observed  
179 seasonal cycle is also required as input to the routing scheme. The model implements mass balance equation at  
180 each time step to calculate storage and outflow/release from the reservoir. The VIC-Res model simulates daily  
181 reservoir inflow, outflow, live storage, and water level. Dang et al. (2019) reported that even the model without a  
182 reservoir exhibits almost the same level of accuracy. However, as the parametrization is inappropriate when the  
183 model is calibrated using the observed flow that is affected by reservoirs, hydrological processes simulated by the  
184 model can be erroneous.

185 We used observed daily precipitation, maximum and minimum temperatures from IMD, and wind speed from  
186 NCEP-NCAR reanalysis as meteorological forcing. We used reservoir storage observations to input the seasonal  
187 cycle for each reservoir into the model. An autocalibration module developed by Dang et al. (2020) was used to  
188 calibrate soil parameters of the VIC-Res model for the Narmada River basin. The autocalibration module uses the  
189  $\varepsilon$ -NSGAII multi-objective evolutionary algorithm (Reed et al., 2013) to adjust the values of sensitive soil  
190 parameters. The autocalibration module can be used to calibrate model parameters at the outlet of different sub-  
191 basins within a river basin. First, we used autocalibration to calibrate parameters of upstream basins, then the  
192 parameters for the downstream basins were calibrated for the grids that are not part of the upstream basins. We  
193 used five soil parameters ( $B_{inf}$ ,  $D_s$ ,  $D_{smax}$ ,  $W_s$ , and depth of three soil layers) to calibrate daily streamflow at the  
194 selected gauge stations in the basin as described in Mishra et al. (2010).  $B_{inf}$  is the variable infiltration curve  
195 parameter.  $D_{smax}$  is the maximum velocity of baseflow.  $D_s$  is a fraction of  $D_{smax}$  where non-linear baseflow begins.  
196  $W_s$  is a fraction of maximum soil moisture non-linear baseflow occurs (Liang et al., 1994). Further details of the  
197 calibration parameters can be obtained from Mishra et al. (2010). The autocalibration module optimizes the  
198 model's performance in simulating streamflow at selected stations considering reservoir dynamics. We set our  
199 objective to maximize Nash-Sutcliffe Efficiency (NSE) [Dawson et al., 2007; Nash and Sutcliffe, 1970]. The  
200 model performance was evaluated for daily streamflow, the water level of reservoirs, and the live storage of

201 reservoirs using NSE and coefficient of determination ( $R^2$ ). Daily streamflow was calibrated and evaluated at  
202 Sandia, Handia, Mandleshwar, and Garudeshwar. We selected different periods for the calibration and evaluation  
203 of the VIC-Res model based on the availability of observed streamflow. For instance, we selected the years 1986-  
204 2000, 1986-2000, 1998-2005, 1998-2005 as the calibration period, while the years 2001-2018, 2001-2018, 2015-  
205 2018, 2015-2018 as the evaluation period for stations Sandia, Handia, Mandleshwar, and Garudeshwar,  
206 respectively. The VIC-Res model performance was also evaluated against water level and live storage for Bargi,  
207 Tawa, Indira Sagar, and Sardar Sarovar reservoirs.

208 We first generated daily meteorological forcing of both ERFS and GEFS forecasts. The ERFS forecast is available  
209 for the extended range (1-32 day lead), while the GEFS forecast is available at 1-10 day lead. We developed  
210 observed initial conditions for each forecast date by forcing the long-term (20 years) observed meteorological  
211 forcing from IMD into the calibrated VIC-Res model. Therefore, the model spin-up is considered in the observed  
212 initial state. We simulated a daily streamflow forecast at all the four selected gauge stations using the  
213 meteorological forcing and initial conditions. The VIC-Res simulations were run for all the ensemble members  
214 for ERFS and GEFS forecasts. The ensemble streamflow forecasts were simulated for 1-32 days lead and ten days  
215 lead for ERFS and GEFS datasets. The ERFS forecast simulations were run for 1-32 days lead with the initial  
216 conditions of every Wednesday generated from VIC-Res model using the observed forcings. Similarly, GEFS  
217 streamflow forecast simulations were performed for 1-10 days lead with initial conditions one day before the  
218 forecast.

### 219 **2.3 Forecast skill evaluation**

220 We evaluated the skills of the streamflow forecast generated using the ERFS and GEFS meteorological forecast  
221 by comparing the simulated streamflow forecast to the observed daily streamflow at each of the four locations.  
222 The model simulated streamflow forecast was evaluated against the VIC-Res model simulated daily streamflow  
223 using the observed forcing due to the unavailability of the observed streamflow for the years 2019-2020. The  
224 ERFS meteorological forcing was used to run the VIC-Res model for 1-32 days from each forecast date using the  
225 initial condition generated using the observed forcing from IMD. Similarly, we ran the GEFS ensemble members  
226 for a 1-10 days lead for each forecast date. We used bias and Normalized Root Mean Square Error (NRMSE) to  
227 evaluate the performance of individual ensemble forecast members, which can be estimated as follows:

$$Bias = \sum_{i=1}^n (Q_{i,i} - Q_{obs,i}) \quad (1)$$

$$NRMSE = \frac{RMSE}{\bar{Q}} \quad (2)$$

where,  $\bar{O}$  = mean of observations.

$$RMSE = \sqrt{\frac{\sum_{i=1}^n (Q_i - Q_{obs,i})^2}{n}} \quad (3)$$

228 where  $Q_{obs,i}$  and  $Q_{sim,i}$  are observed and simulated streamflow, respectively. Bias provides a measure of  
 229 correspondence between the mean of observations and the mean of the VIC-Res model simulations, while NRMSE  
 230 represents the relative magnitude of the squared error. We also evaluated the skills of ERFS forecast using  
 231 Continuous Ranked Probability Score (CRPS) [Hersbach, 2000], which measures the closeness between the  
 232 distributions of forecast and observations. The CRPS can be estimated as follows:

$$233 \quad CRPS(F, x) = \int_{-\infty}^{\infty} (F(y) - H(y - x))^2 dy \quad (4)$$

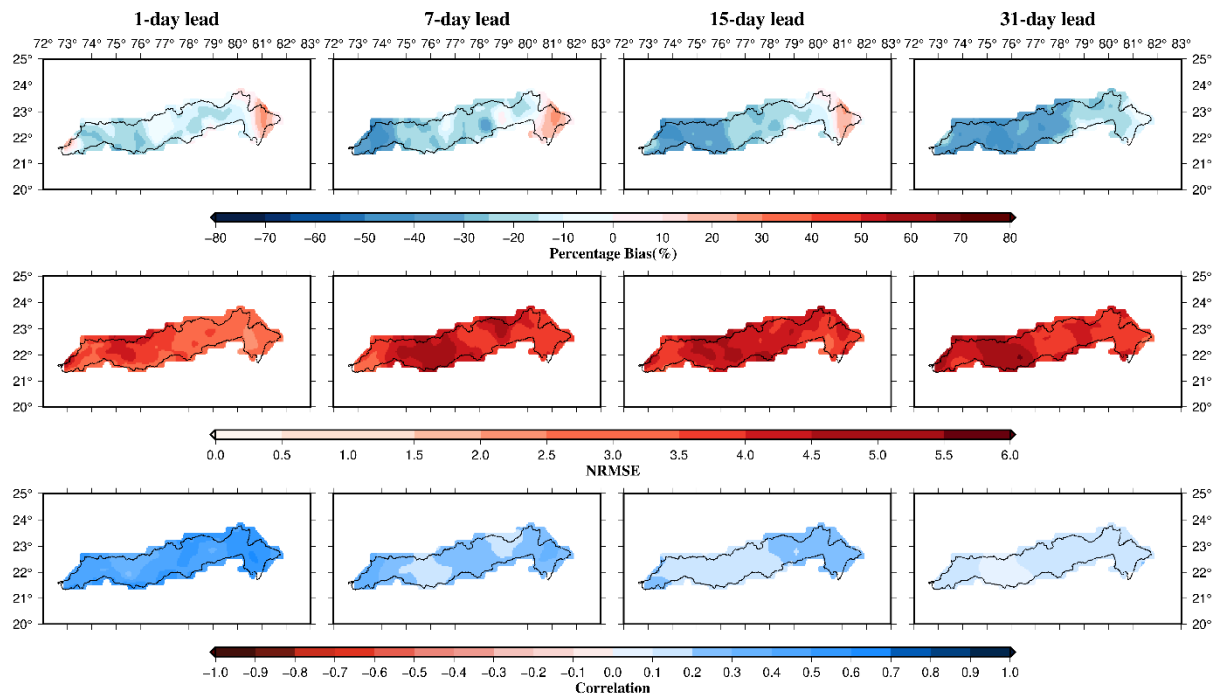
234 where  $F(x)$  is the cumulative distribution function (CDF) associated with probabilistic forecast and  $H(x)$  is the  
 235 Heaviside function ( $H(x) = 1$  for  $x \geq 0$  and zero otherwise). The unit of CRPS is the same of observations.  
 236 Gneiting and Raftery (2007) suggested CRPS as a direct measure to compare deterministic and probabilistic  
 237 forecasts.

### 238 3 Results

#### 239 3.1 Skill evaluation of ERFS and GEFS meteorological forecasts

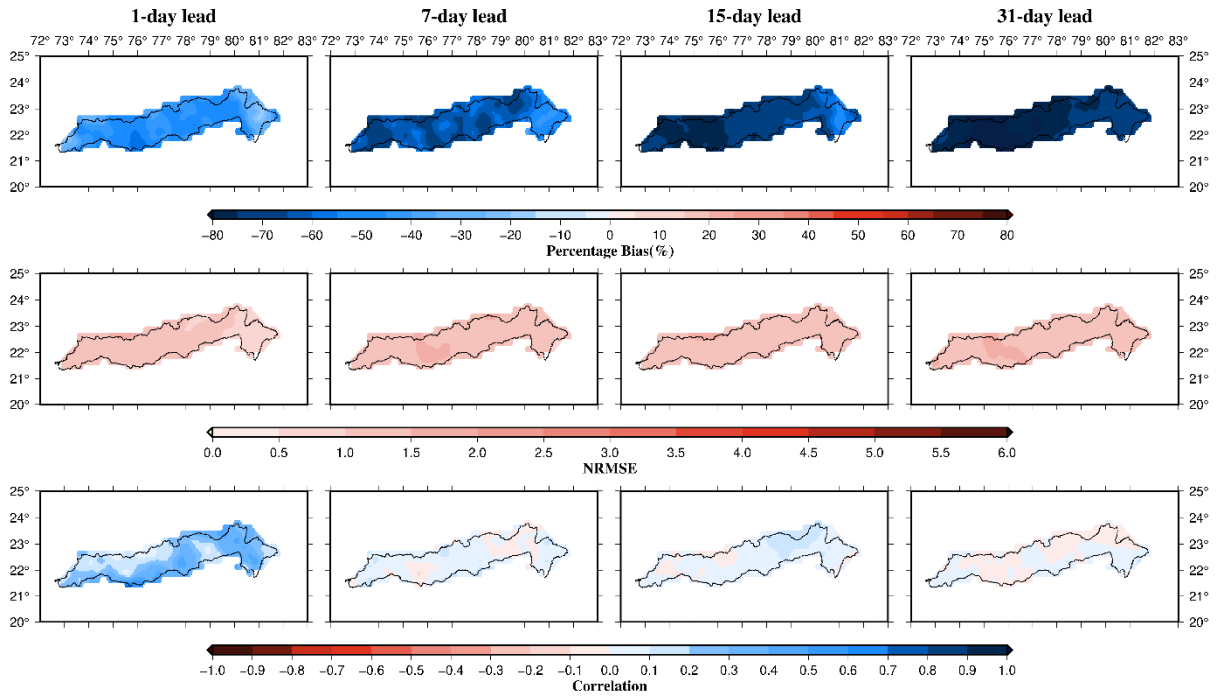
240 First, we evaluated ERFS precipitation and temperature forecast skills for 1-, 7-, 15-, and 31-day leads. We used  
 241 bias, NRMSE, and correlation coefficient ( $r$ ) to estimate the forecast skills. The forecast skill was evaluated for  
 242 the period 2003-2018. We estimated the forecast skill for each ensemble member and then calculated the median  
 243 of the forecast skill of all the sixteen members for each grid in the Narmada river basin. Precipitation forecast from  
 244 ERFS shows a negative bias indicating an underestimation compared to observed rainfall. The dry bias in  
 245 precipitation forecast increases with the lead time (Fig. 2). For the 1-day lead, precipitation forecast from ERFS  
 246 showed a moderate positive correlation (median  $\sim 0.49$ ), which declines with the lead time. Similarly, NRMSE in  
 247 precipitation forecast is large ( $>2.0$ ) over the river basin. We also estimated bias in the precipitation forecast  
 248 exceeding the 90<sup>th</sup> percentile (Fig. 3). The extreme rainfall in the raw ERFS forecast dataset exhibited a weaker  
 249 correlation with the observed extreme precipitation. Moreover, a considerable dry bias in the extreme precipitation  
 250 forecast was found. We also evaluated forecast skills for maximum and minimum temperature against the observed  
 251 temperatures from IMD for the 2003-2018 period (Fig. S1 and S2). The daily temperature forecast showed a  
 252 relatively higher positive correlation with the observed temperatures from IMD. Moreover, lower NRMSE was

253 noted for the temperature forecast than the observed maximum and minimum temperatures. However, a positive  
254 bias of  $\sim 1.5$   $^{\circ}\text{C}$  (median of all grids in the basin) was found in minimum temperature forecast at all the lead times.



255  
256 **Figure 2. Evaluation of ERFS precipitation forecast against observations for the 2003-2018 period. Forecast skills**  
257 **were evaluated using bias, NRMSE, and correlation for each ensemble member and the median skill is presented.**

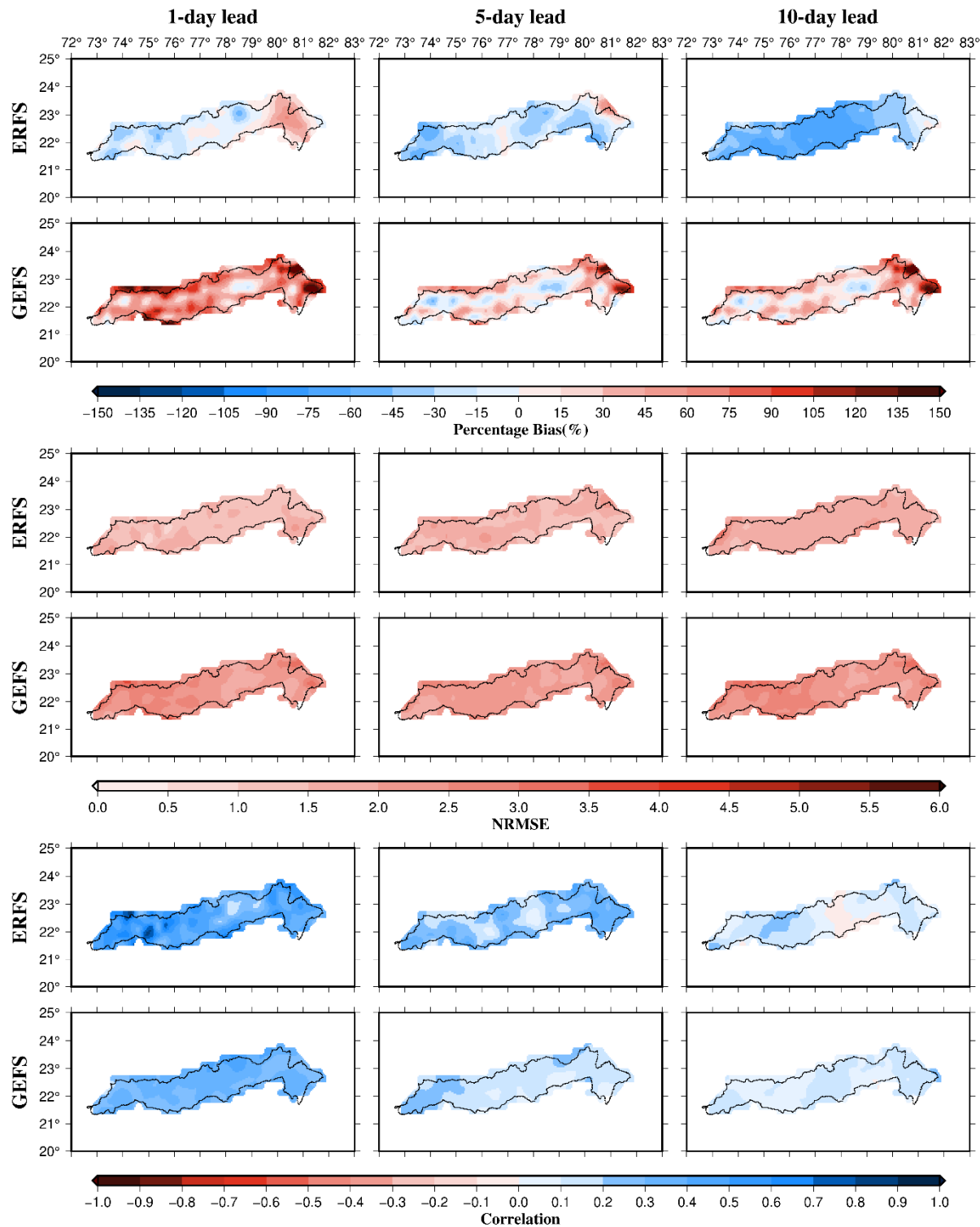
258



259

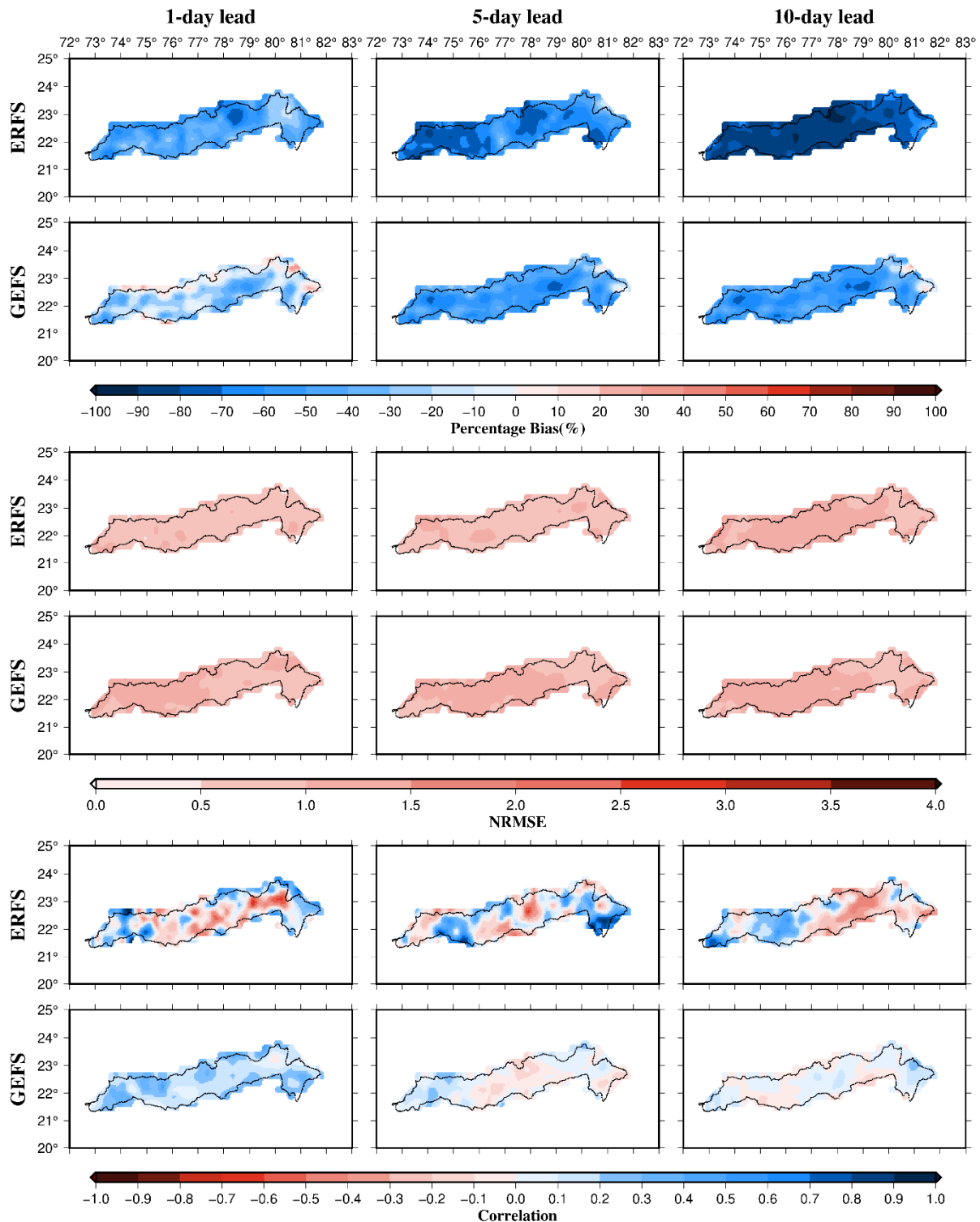
260 **Figure 3, Evaluation of extreme precipitation (>90th percentile) forecast skill from ERFS for the 2003-2018 period.**  
 261 Forecast skills were evaluated using bias, NRMSE, and correlation for each ensemble member and the median skill is  
 262 presented.

263 Next, we compared the ERFS and GEFS ensemble forecast skills for the summer monsoon (June-September) of  
 264 the 2019-2020 period. We limit the comparison to the two years as the GEFS ensemble forecast is available only  
 265 for 2019-2020. We evaluated forecast skills for 1-, 5-, and 10-day leads (Fig. 4). Our results show that the ERFS  
 266 precipitation forecast has a dry bias across the river basin and all the leads (Fig 4). The GEFS precipitation forecast  
 267 showed a positive (wet) bias in the majority of the Narmada river basin. The forecast products (ERFS and GEFS)  
 268 underestimate extreme rainfall in the Narmada basin (Fig 5). The dry bias in extreme rainfall increases with lead  
 269 time in the ERFS and GEFS forecasts (Fig. 5). The forecast products showed a poor correlation with the observed  
 270 extreme precipitation in the Narmada river basin (Fig. 5). However, both the forecast products demonstrated  
 271 relatively better skills for maximum and minimum temperatures than precipitation (Fig. S3 and S4).



272

273 **Figure 4. Comparison of the precipitation forecast skills from ERFS and GEFS for the summer monsoon period**  
 274 **during 2019-2020. Forecast skills were evaluated using bias, NRMSE, and correlation for each ensemble member of**  
 275 **ERFS and GEFS and the median skill is presented.**



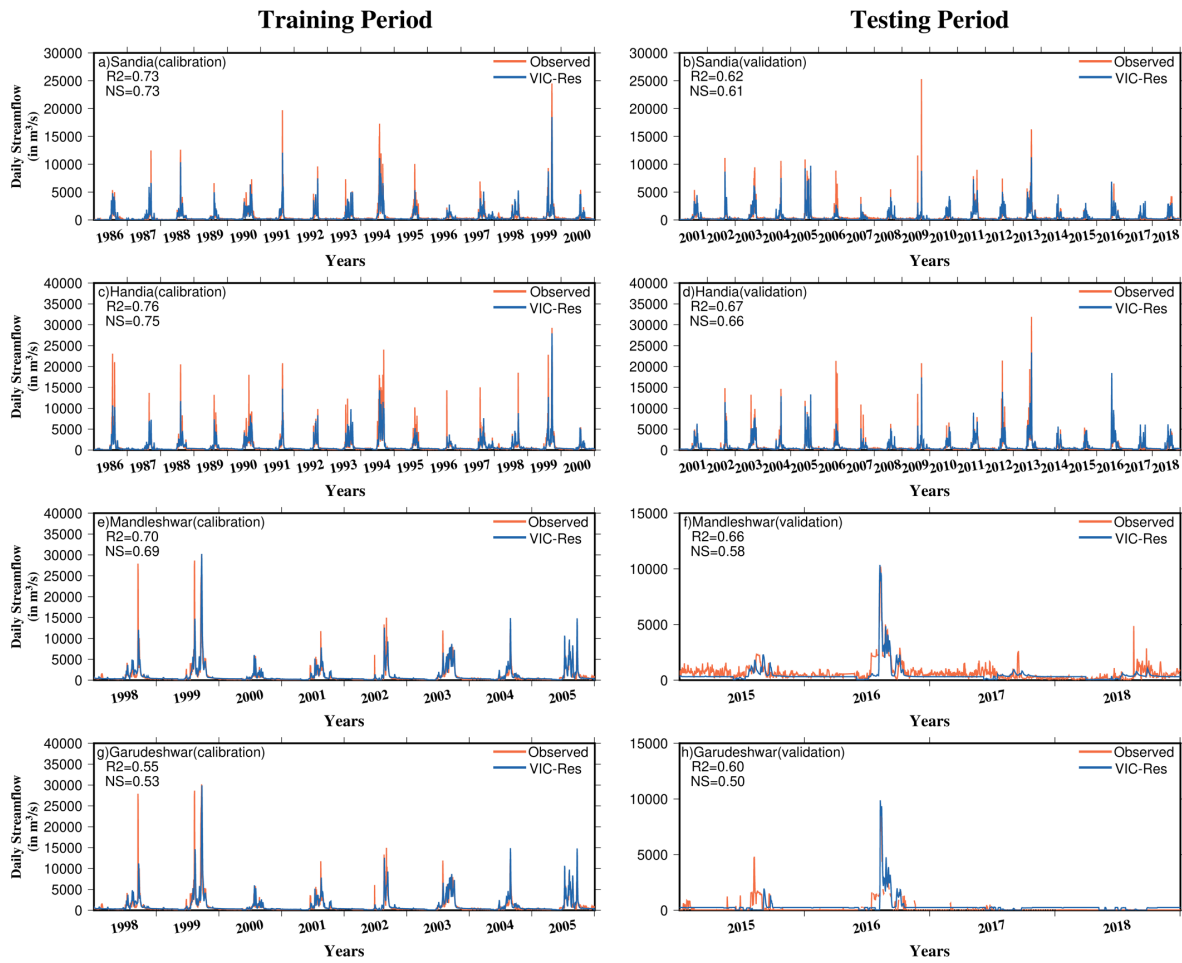
276

277 **Figure 5.** Comparison of the extreme precipitation (exceeding 75<sup>th</sup> percentile) forecast skills from ERFS and GEFS for  
 278 the summer monsoon period during 2019-2020. Forecast skills were evaluated using bias, NRMSE, and correlation  
 279 for each ensemble member of ERFS and GEFS and the median skill is presented.

280

281 **3.2 Calibration and evaluation of the VIC-Res model**

282 We performed calibration of reservoir level and storage and calibration of daily streamflow. Daily storage and  
283 water level calibrated the VIC-Res model for four major reservoirs (Bargi, Tawa, Indira Sagar and Sardar Sarovar)  
284 in the Narmada basin. The upstream catchment area of all the gauge locations and calibration parameters are shown  
285 in supplementary Figure S5. We evaluated the VIC-Res model's performance using the coefficient of  
286 determination ( $R^2$ ) and Nash Sutcliffe Efficiency (NSE) (Fig. 6). The VIC-Res model simulates daily streamflow  
287 at the selected stations in the basin.  $R^2$  and NSE values were above 0.65 at Sandia, Handia, and Mandleshwar  
288 stations for the calibration period. While at Garudeshwar, the VIC-Res model performed comparatively weaker  
289 ( $R^2 = 0.55$  & NSE = 0.53) for the calibration period.



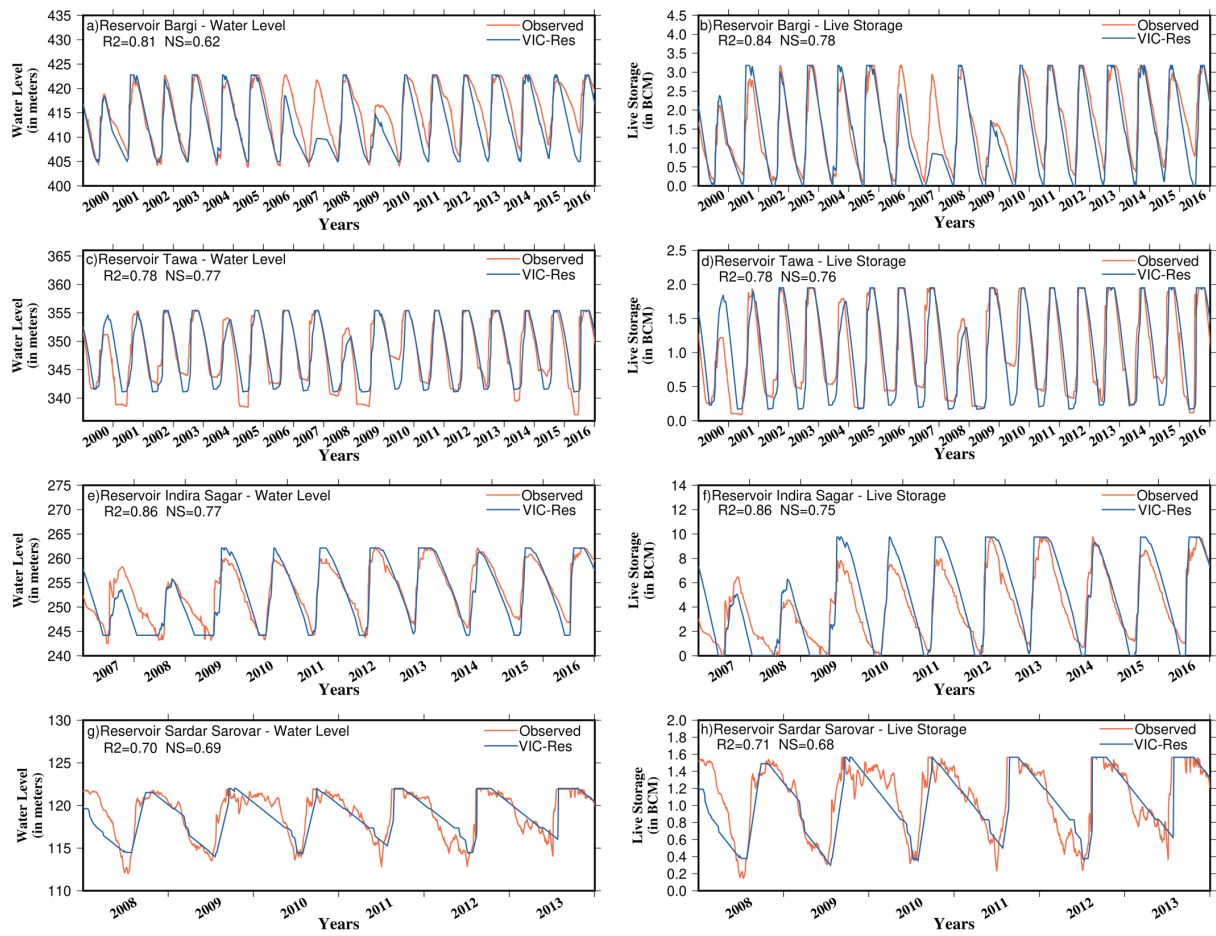
290

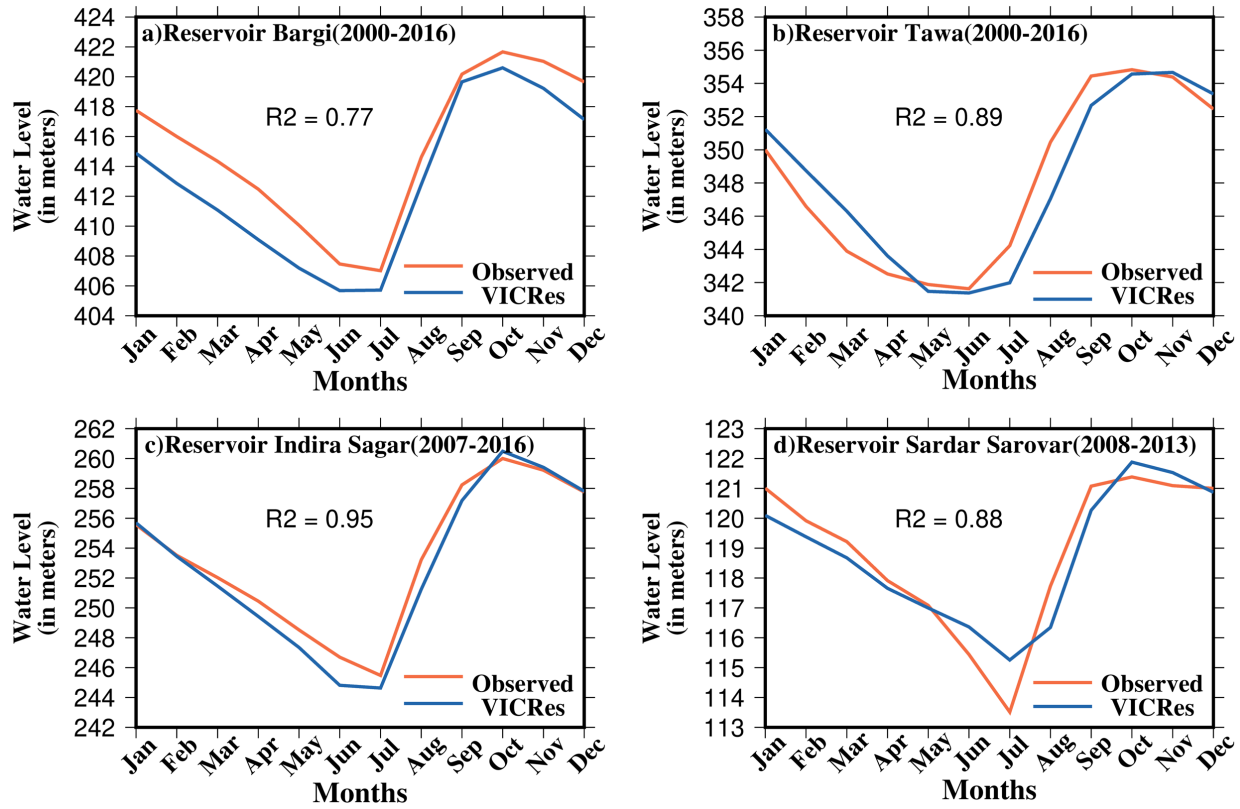
291 **Figure 6. Calibration and evaluation of the VIC-Res model against observed daily streamflow at**  
 292 **Sandia, Handia, Mandleshwar and Garudeshwar. The performance of the VIC-Res model in simulating daily**  
 293 **streamflow was evaluated using the  $R^2$  and NSE.**

294

295 We considered the influence of major reservoirs on the simulated daily streamflow. Therefore, the VIC-Res  
 296 model's performance in simulating daily reservoir storage and the water level was evaluated against the streamflow  
 297 observations. We selected 2000-2016, 2000-2016, 2007-2016, and 2008-2013 as evaluation periods for Bargi,  
 298 Tawa, Indira Sagar, and Sardar Sarovar reservoirs, respectively, based on the availability of observations. We  
 299 estimated  $R^2$  and NSE to evaluate the model's performance (Fig. 7). The model performed well in simulating all  
 300 the reservoirs' water levels and storage ( $R^2 > 0.78$  and  $NSE > 0.62$ ). We also compared the seasonal cycle of the  
 301 observed and simulated reservoir storage for all the four major reservoirs (Fig. 8). The model simulated monthly  
 302 seasonal cycle of reservoir storage compares well with the observed storage for all the dams with  $R^2$  of more than  
 303 0.77. We find that the model underestimates storage for Bargi reservoir, which can be due to relatively smaller

304 upstream catchment area that may not capture the spatial variability of rainfall. Overall, we find that the VIC-Res  
 305 model can evaluate the ensemble streamflow forecast in the Narmada river basin.

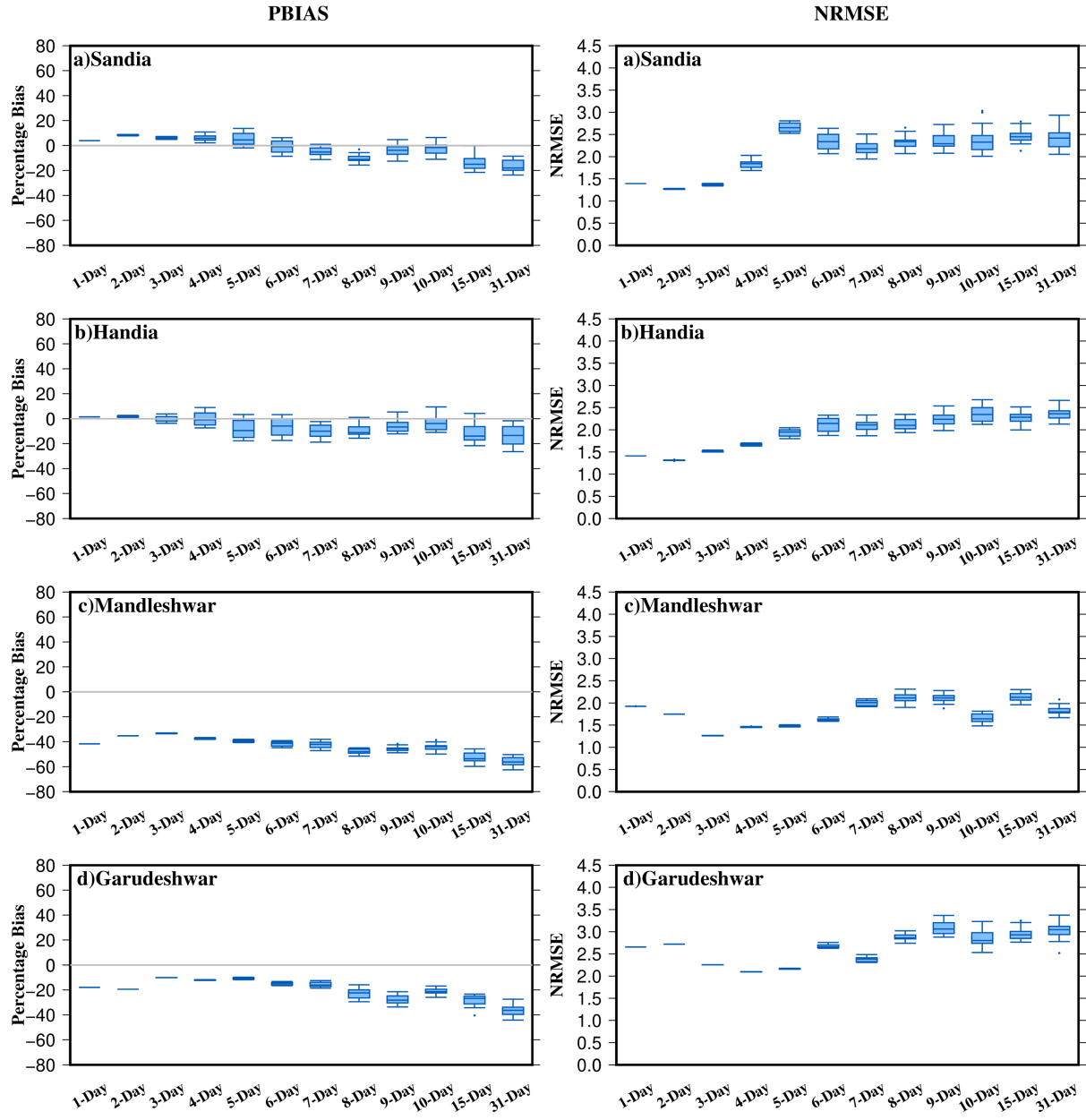




310 **Figure 8. Comparison of observed and the VIC-Res model simulated reservoir water levels for four reservoirs in  
311 Narmada River basin.**

### 312 3.3 Evaluation of ensemble streamflow forecast skills of ERFS

313 We estimated forecast skills of daily streamflow for 2003-2018 generated from each ensemble member of ERFS  
314 for the twelve lead times (1-day to 10-day, 15-day, and 31-day). We selected a 1-10 day lead as GEFS forecast is  
315 also available with the same lead. In addition, two other lead times (15 and 31 days) were selected to evaluate the  
316 forecast skill of streamflow forecast from all the sixteen members of ERFS (Fig. 9). Both bias and NRMSE showed  
317 a relatively lesser spread for the shorter lead (1-3 day) streamflow forecast from all the ensemble members of  
318 ERFS (Fig. 9). However, uncertainty in streamflow forecast due to different ensemble members increases with the  
319 lead time. NRMSE of streamflow forecast from ERFS also rises with the lead at all the stations. Ensemble  
320 streamflow forecast from ERFS showed a positive bias for Sandia, Handia, and Garudeshwar, while a negative  
321 bias was found for Mandleshwar station (Fig. 9). We estimated the CRPS, which is higher for 1-day lead compared  
322 to 3-day leads and increases with the lead time (Figure S6).



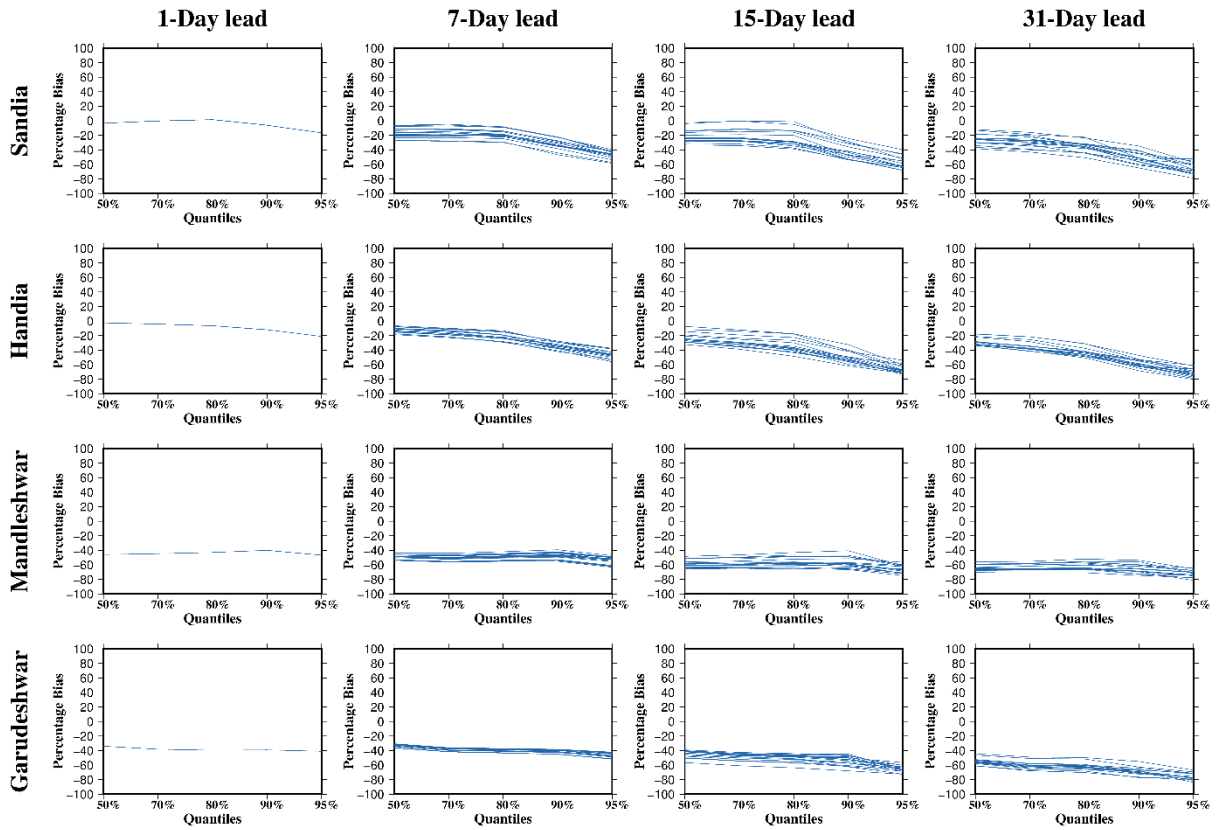
323

324 **Figure 9. Ensemble streamflow forecast skill based on the ERFS forecast for 2003-2018.** The forecast was evaluated  
 325 using bias (%) and NRMSE. Box and whisker plots show the skill for all 16 ensemble members at lead 1-10 day, 15  
 326 day and 31 days at four gauge stations.

327

328 We estimated the forecast skill in streamflow exceeding certain thresholds (50,70,80,90, and 95<sup>th</sup> percentiles) [Fig.  
 329 10]. We find less spread in bias among different ensemble members for 1-day lead streamflow forecast from ERFS.  
 330 However, the spread of bias in streamflow forecast due to different ensemble members increases with the lead

331 time (Fig. 10). Moreover, bias in streamflow forecast remains stable for all the selected percentile thresholds at a  
 332 1-day lead at all the four-gauge stations. On the other hand, bias in streamflow forecast increases for higher  
 333 percentiles at longer lead times. For instance, dry bias in streamflow forecast in all the ensemble members is higher  
 334 for the 95<sup>th</sup> percentile than for the 50<sup>th</sup> percentile. Therefore, our results show that regardless of the spread among  
 335 the ensemble members from ERFS, almost all the ensemble members underestimate the high flow at all the gauge  
 336 stations in the Narmada river basin (Fig. 10).



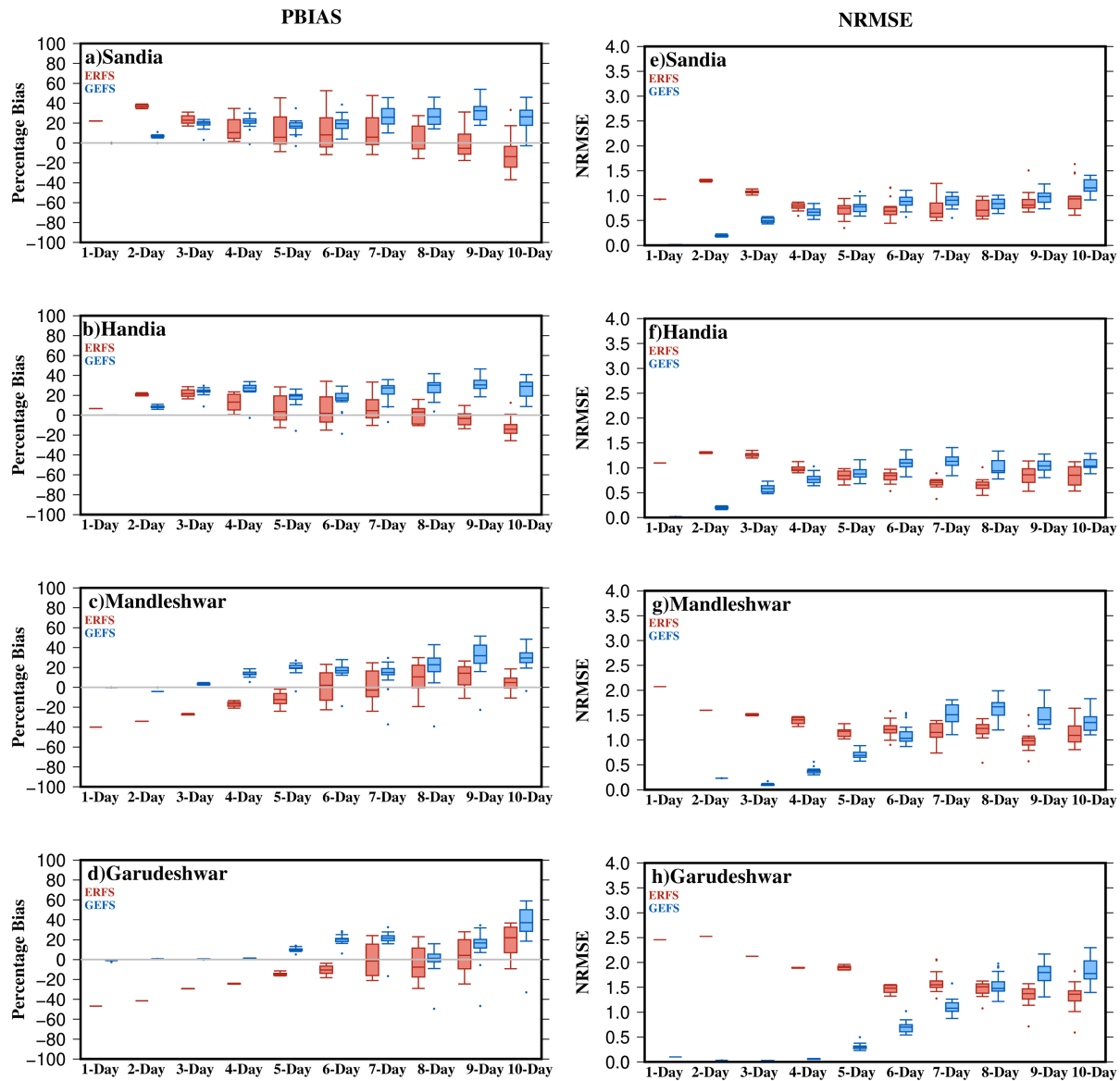
337

338 **Figure 10. Bias in ensemble streamflow forecast estimated using ERFS for 2003-2018 for streamflow percentiles**  
 339 **exceeding 50<sup>th</sup>, 70<sup>th</sup>, 80<sup>th</sup>, 90<sup>th</sup>, and 95<sup>th</sup> thresholds. Bias in ensemble streamflow forecast was evaluated at 1, 7, 15, and**  
 340 **31 day lead.**

### 341 3.4 Comparison of ensemble streamflow forecast skills ERFS and GEFS

342 We compared the streamflow forecast skills of 16 ensemble members from ERFS and 21 ensemble members from  
 343 GEFS. Since GEFS meteorological forecast is available only for 2019-2020, we compared the summer monsoon  
 344 season of these two years. ERFS forecast is available weekly for 1-32 days, while the GEFS forecast is generated  
 345 every day. Therefore, we compared the daily streamflow forecast from both the products for the weeks for which  
 346 the ERFS forecast was available for the summer monsoon of the 2019-2020 period. We compared the streamflow  
 347 forecast skills for all the ensemble members at 1 to 10 day leads at Sandia, Handia, Mandleshwar, and Garudeshwar

348 (Fig. 11). We find that the GEFS forecast has a better skill for the short lead time (~1-5 days) with less bias and  
 349 NRMSE. On the other hand, the ERFS ensemble forecast showed higher bias and NRMSE at shorter leads for  
 350 most of the selected locations in the Narmada basin. Streamflow forecast skill of GEFS declines rapidly after the  
 351 3-4 day lead time for most of the locations in the Narmada basin. The forecast products showed a larger spread  
 352 among the streamflow forecast ensemble members after five days lead. For short to medium range (~1 to 5 days),  
 353 the streamflow forecast from GEFS performed better with low NRMSE and bias for streamflow exceeding the  
 354 75<sup>th</sup> percentile of the summer monsoon period (Fig. S7). Moreover, streamflow forecast skill from the ERFS was  
 355 considerably lower than the GEFS at most of the locations for flow exceeding 75<sup>th</sup> percentiles (Fig. S7).

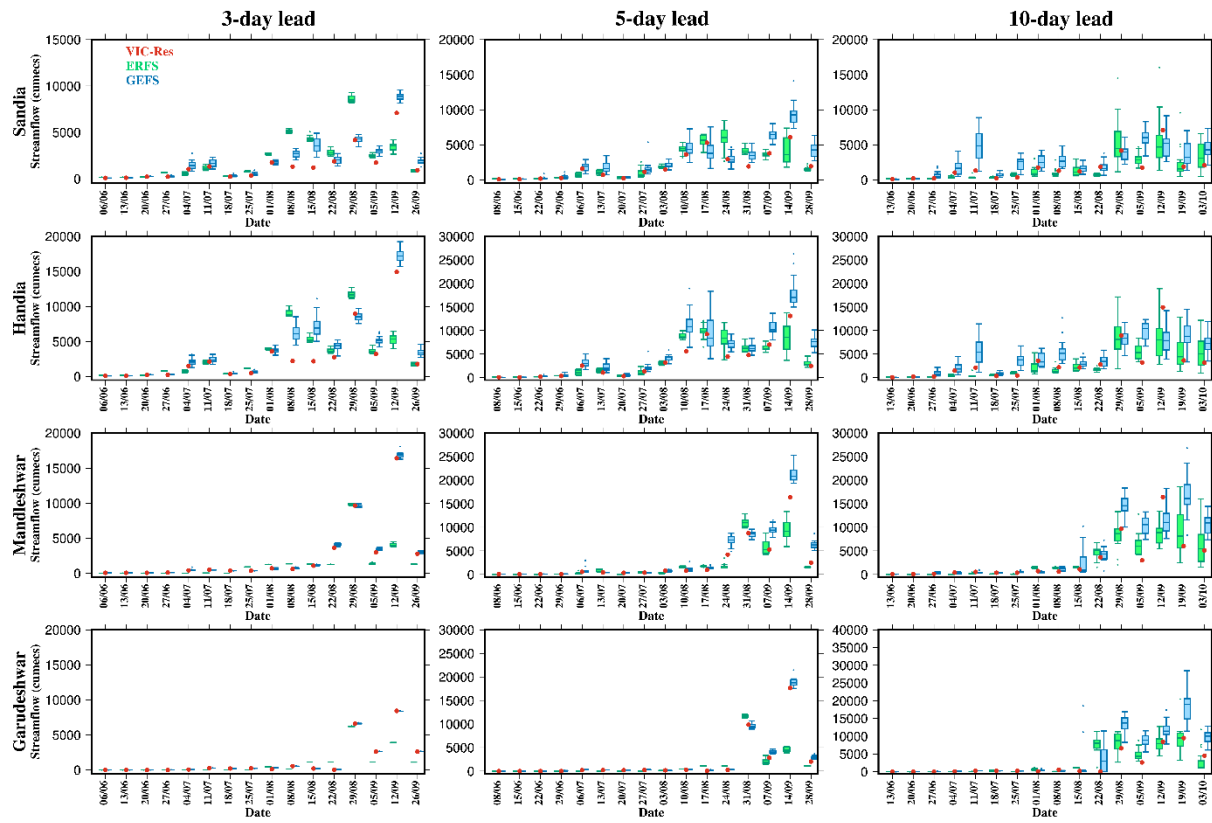


356

357 **Figure 11. Comparison of ensemble streamflow forecast skills from ERFS and GEFS for 2019-2020. The forecast skill**  
 358 **was evaluated considering the VIC-Res simulated streamflow with the observed forcing from IMD due to**  
 359 **unavailability of observed flow.**

360 We examined the daily streamflow forecast skill at 3-day, 5-day, and 10-leads from ERFS and GEFS forecasts for  
 361 the summer monsoon season of 2019 & 2020 against VIC-Res simulated streamflow using the observed  
 362 meteorological forcing at all the four gauge stations (Fig. 12 and Fig. S8). Since observed daily streamflow was  
 363 unavailable for skill assessment, the comparison was made against the VIC model simulated flow with the  
 364 observed meteorological forcing (Fig. 12 and Fig. S8). The GEFS forecast successfully captured streamflow peaks  
 365 in both 2019 and 2020 at a 3-day lead. In 2019, GEFS forecasts overestimated streamflow peaks at 3-day and 5-  
 366 day leads during the summer monsoon. On the other hand, the ensemble streamflow forecast developed using the  
 367 ERFS meteorological forecast showed a higher spread than GEFS (Fig. 12, Fig. S8). The spread in ensemble  
 368 streamflow forecast increases for both ERFS and GEFS forecast at a 10-day lead. However, the ERFS's streamflow  
 369 forecast showed a better skill at the 10-day lead. Despite having fewer ensemble members than the GEFS, the  
 370 ERFS forecast showed a broader spread in streamflow prediction, highlighting a higher uncertainty in prediction.  
 371 We find that GEFS overestimate streamflow the ERFS underestimates most of the locations and lead times.

372

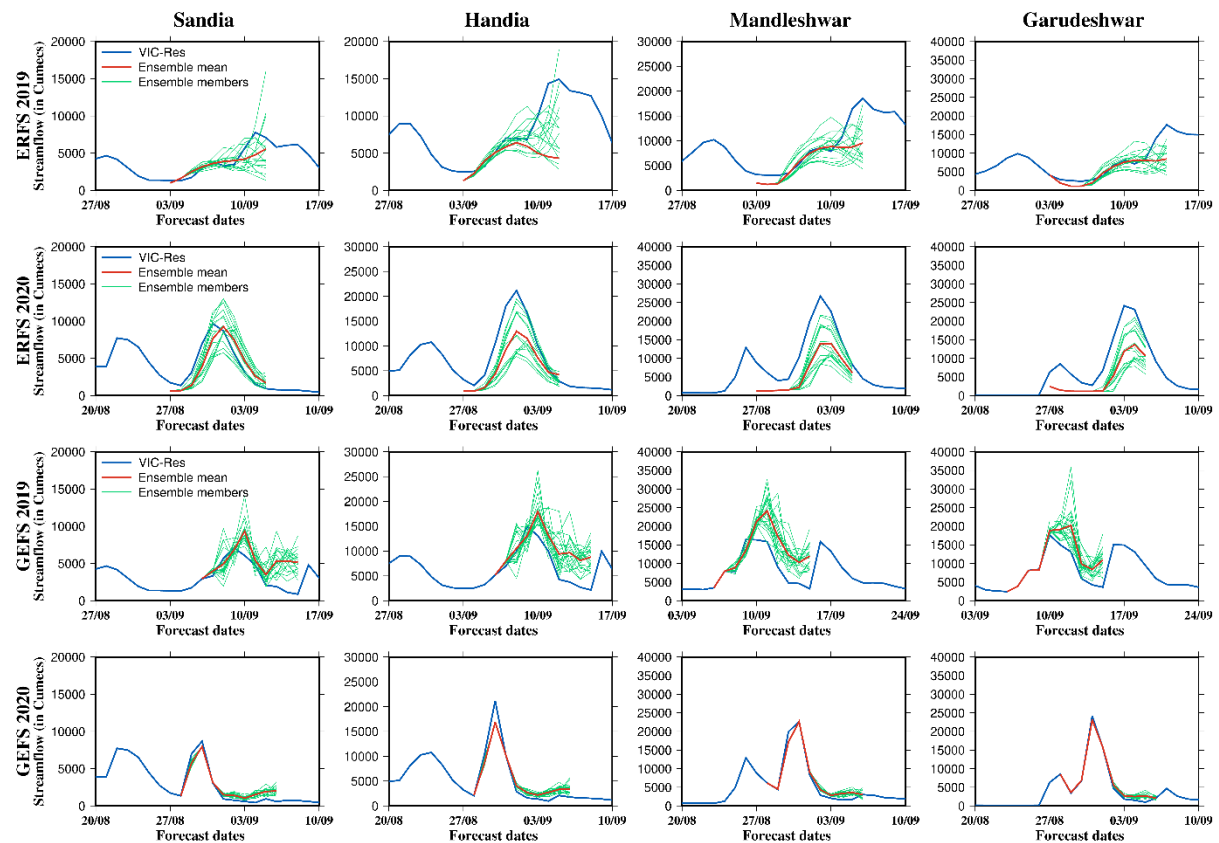


373

374 **Figure 12. Comparison of ensemble streamflow simulated using the VIC-Res model with ERFS and GEFS forecast**  
 375 **products during the summer monsoon of 2019. The forecast skill was evaluated considering the VIC-Res simulated**  
 376 **streamflow with the observed forcing from IMD due to unavailability of observed flow.**

377

378 We examined the streamflow forecast generated by all the ensemble members of ERFS and GEFS for a few events  
 379 using the VIC-Res model (Fig. 13). The ensemble streamflow prediction was compared considering the model  
 380 simulated streamflow with the observed forcing from IMD. In 2019, the ensemble mean streamflow from all the  
 381 ensemble members of ERFS considerably underestimated the peak flow (Fig. 13). However, a few ensemble  
 382 members of the ERFS forecast captured the peak flow at the four locations of the Narmada river basin (Fig. 13).  
 383 At Handia station, 1 out of 16 ensemble members exceeds the observed streamflow. Moreover, GEFS forecasts at  
 384 short leads (3-5 days) performed well in capturing peaks (Fig. 13). However, GEFS forecasts showed a smaller  
 385 spread in ensemble streamflow at the short lead time (1-5 days). Overall, we find that ensemble forecasts can be  
 386 used for probabilistic streamflow prediction.



387  
 388 **Figure 13. Ensemble streamflow simulations using the ERFS forecast at 5-11 day lead and GEFS forecast at 3-5 day**  
 389 **lead against the VIC-Res simulated streamflow with the observed meteorological forcing for 2019 and 2020.**

390

391 **4 Discussion and conclusions**

392 Streamflow forecast plays an essential role in efficient reservoir operations and flood mitigation (Chen et al., 2016;  
393 Mediero et al., 2007). A reliable streamflow forecast can reduce uncertainty in reservoir operations and enhance  
394 the development of a flood early warning system. Notwithstanding the considerable progress in an operational  
395 meteorological forecast from different agencies, efforts to establish an ensemble streamflow forecast system at  
396 river basin scales have been limited for India. Moreover, it remains unclear if other meteorological forecast  
397 products have different streamflow forecast skills. We used the two meteorological ensemble forecast products  
398 from IMD to examine streamflow forecast skills in the Narmada river basin. The presence of reservoirs influence  
399 the water budget and streamflow (Shah et al., 2019 Zajac et al., 2017; Yun et al., 2020; Chai et al., 2019).  
400 Hydrological model parameters calibrated without considering the role of reservoirs can be erroneous and leading  
401 to errors and uncertainty in simulated hydrological processes (Dang et al., 2019). Therefore, we used the ensemble  
402 streamflow prediction approach to generate the daily streamflow simulations considering the influence of  
403 reservoirs in the Narmada river basin. We compared the performance of ERFS and GEFS ensembles for the  
404 summer monsoon period of 2019-20. We also assessed the skills of the ERFS dataset solely for a more extended  
405 period from 2003 to 2018.

406 The ERFS ensemble forecast is available once a week at 1-32 days lead time. On the other hand, GEFS ensemble  
407 forecasts are available daily at 1-10 days lead for the summer monsoon period of 2019-2020. Hagedorn et al.  
408 (2005) reported that bias-correction of the raw forecast does not necessarily increase the forecast skill. Moreover,  
409 statistical correction of the raw forecast is inappropriate, which can lose its effect propagating through the  
410 hydrological model (Zalachori et al., 2012; Crochemore et al., 2016; Benninga et al., 2017; Hagedorn et al., 2005).  
411 Therefore, we did not bias-correct the raw meteorological ensemble forecasts from ERFS and GEFS. The skills of  
412 ERFS and GEFS precipitation and temperature (minimum and maximum) forecasts were estimated for 1-, 5- and  
413 10-day lead. The GEFS raw forecast showed better skills than the ERFS forecast for mean and extreme  
414 precipitation. As precipitation plays a vital role in streamflow forecast (Meaurio et al., 2017; Demargne et al.,  
415 2014; Pappenberger et al., 2005), our results show that GEFS forecast provides better skills for streamflow  
416 prediction in the Narmada River basin. The post-processing of streamflow data can significantly improve  
417 performance (Tiwari et al., 2021; Muhammad et al., 2018), which can be used in the future to examine the  
418 improvements in streamflow prediction. Moreover, a multi-model approach can be used to reduce the errors and  
419 uncertainty in streamflow forecasts that could arise due to the parameterization of hydrological models (Velázquez  
420 et al., 2011; Zarzar et al., 2018; Muhammad et al., 2018).

421 The skills of ERFS and GEFS ensemble forecasts were estimated for 1, 5 and 10-day leads. GEFS raw forecasts  
422 illustrated better skills than ERFS forecasts for overall rainfall and extreme precipitation. As studies show that rain  
423 plays a vital role in streamflow forecast (Demargne et al., 2014; Meaurio et al., 2017; Pappenberger et al., 2005),

424 we also observed the same results. The ensemble forecast with better skills performed well in predicting daily  
425 streamflow. Correcting the bias of the input forecast may shrink the variability range of the result. However,  
426 ensemble forecasts aim to capture uncertainties. Studies suggest that the post-processing of streamflow data can  
427 significantly improve performance (Muhammad et al., 2018; Tiwari et al., 2021). A multi-model approach, where  
428 more than one hydrological model is used, can generalize the uncertainty introduced by the hydrological model.  
429 Various studies have reported improved forecast skills using the multi-model approach (Muhammad et al., 2018;  
430 Velázquez et al., 2011; Zarzar et al., 2018). Also, our analysis is based on just for the 2019-2020 as the GEFS  
431 hindcast is available only for this period. Availability of longer hindcast from the GEFS can help to understand  
432 the forecast skills for hydrological extremes (drought and floods). Moreover, we did not examine the forecast skill  
433 of reservoir storage, which can provide a better understanding of the impacts of storage during the floods.

434 Flood forecasting using the available meteorological forecast products can help in mitigating the losses through  
435 early warnings. To account for the uncertainty arising from initial state and model parameterization, the individual  
436 members of the ensemble weather forecast can provide better information than their ensemble mean (Saleh et al.,  
437 2019). The probabilistic approach over the deterministic method provides the range of variability, which can help  
438 determine the probability of exceeding a specific threshold of streamflow (Hsiao et al., 2013). The shift from the  
439 existing 'flood forecast system' to the 'ensemble-based probabilistic forecast' requires modifications in the current  
440 flood forecast practice. The transition is expected to change various aspects of the existing decision-making  
441 process. The forecasters need to train the on-duty officers adequately and the authorities on probabilistic forecasts.  
442 We evaluated the streamflow forecast skills at 1-32 day lead in the Narmada river basin. The increased lead time  
443 in streamflow forecast can assist in developing efficient communication methods of information (Arnal et al.,  
444 2020; Ramos et al., 2010). Moreover, ensemble streamflow forecast at longer leads can be effectively used in  
445 optimizing reservoir operations (Alemu et al., 2011). Our results show that, while the mean of the ensemble  
446 members failed to capture the high flows, a few individual ensemble members performed better in capturing peak  
447 flow, which can be used to develop probabilistic early warnings.

448 Based on our findings, the following conclusions can be made:

- 449 1) The raw precipitation forecast from both GEFS and ERFS datasets showed moderate skills (bias, NRMSE  
450 and correlation) against observations from IMD at 1-day, 5-day and 10-day lead times. While both (ERFS  
451 and GEFS) forecast products underestimated extreme precipitation, dry bias in the ERFS forecast was  
452 more prominent than the GEFS forecast. For instance, raw precipitation forecast from ERFS showed  
453 negative bias across the Narmada river basin. On the other hand, the raw precipitation forecast from GEFS  
454 exhibited both negative and positive bias. Both the forecast products showed better skills for maximum  
455 and minimum temperatures than precipitation.
- 456 2) We calibrated and evaluated the VIC-Res model to simulate streamflow, considering the influence of  
457 reservoirs at four gauge stations in the Narmada River Basin. The model reproduced daily streamflow,  
458 reservoir water level, and storage reasonably well against the observations.

459 3) Comparing the streamflow forecast skills of both the ensemble forecasts showed that GEFS forecasts  
460 performed better than the ERFS at all the locations in the basin. However, both the forecast products  
461 underestimated the extremes, which can be due to dry bias in extreme precipitation. The spread in  
462 streamflow due to different ensemble members increased with the forecast lead time. Overall, an  
463 ensemble forecast can be used to develop a probabilistic forecast based flood early warning system.

464 **Data availability:** All the datasets used in this study can be obtained from the corresponding author.

465

466 **Competing interest:** Authors declare no competing interest.

467 **Author contributions:** VM designed the study. UV conducted simulations and wrote the first draft. UV and  
468 VM discussed the results and prepared the final version.

469 **Acknowledgement:** The work was supported by the Monsoon Mission, Ministry of Earth Sciences. The authors  
470 acknowledge the data availability from India Meteorological Department (IMD) and India-WRIS. ERFS and  
471 GEFS forecast products were obtained from the Indian Institute of Tropical Meteorology (IITM), Pune.

472 **References**

473 Alemu, E. T., Palmer, R. N., Polebitski, A., and Meaker, B.: Decision Support System for Optimizing Reservoir  
474 Operations Using Ensemble Streamflow Predictions, *J Water Resour Plan Manag*, 137, 72–82,  
475 [https://doi.org/10.1061/\(asce\)wr.1943-5452.0000088](https://doi.org/10.1061/(asce)wr.1943-5452.0000088), 2011.

476 Alfieri, L., Burek, P., Dutra, E., Krzeminski, B., Muraro, D., Thielen, J., and Pappenberger, F.: GloFAS-global  
477 ensemble streamflow forecasting and flood early warning, *Hydrol Earth Syst Sci*, 17, 1161–1175,  
478 <https://doi.org/10.5194/hess-17-1161-2013>, 2013.

479 Ali, H., Modi, P., and Mishra, V.: Increased flood risk in Indian sub-continent under the warming climate,  
480 *Weather Clim Extrem*, 25, <https://doi.org/10.1016/j.wace.2019.100212>, 2019.

481 Arnal, L., Anspoks, L., Manson, S., Neumann, J., Norton, T., Stephens, E., Wolfenden, L., and Cloke, H. L.: “  
482 Are we talking just a bit of water out of bank? Or is it Armageddon?” Front line perspectives on transitioning to  
483 probabilistic fluvial flood forecasts in England, 203–232, <https://doi.org/https://doi.org/10.5194/gc-3-203-2020>,  
484 2020.

485 Benninga, H. F., Booij, M. J., Romanowicz, R. J., and Rientjes, T. H. M.: Performance of ensemble streamflow  
486 forecasts under varied hydrometeorological conditions, 5273–5291, <https://doi.org/https://doi.org/10.5194/hess-21-5273-2017>, 2017.

488 Boulange Julien and Hanasaki Naota: A global flood risk analysis with explicit representation of major dams,  
489 [https://doi.org/https://doi.org/10.11520/jshwr.32.0\\_12](https://doi.org/https://doi.org/10.11520/jshwr.32.0_12), 2013.

490 Bowler, N. E., Arribas, A., Mylne, K. R., Robertson, K. B., and Beare, S. E.: The MOGREPS short-range  
491 ensemble prediction system, 722, 703–722, <https://doi.org/10.1002/qj>, 2008.

492 Chai, Y., Li, Y., Yang, Y., Zhu, B., Li, S., Xu, C., and Liu, C.: Influence of Climate Variability and Reservoir  
493 Operation on Streamflow in the Yangtze River, *Sci Rep*, 9, <https://doi.org/10.1038/s41598-019-41583-6>, 2019.

494 Chen, L., Singh, V. P., Lu, W., Zhang, J., Zhou, J., and Guo, S.: Streamflow forecast uncertainty evolution and  
495 its effect on real-time reservoir operation, *J Hydrol (Amst)*, 540, 712–726,  
496 <https://doi.org/10.1016/j.jhydrol.2016.06.015>, 2016.

497 Cloke, H. L. and Pappenberger, F.: Ensemble flood forecasting : A review, *J Hydrol (Amst)*, 375, 613–626,  
498 <https://doi.org/10.1016/j.jhydrol.2009.06.005>, 2009.

499 Crochemore, L., Ramos, M. H., and Pappenberger, F.: Bias correcting precipitation forecasts to improve the skill  
500 of seasonal streamflow forecasts, *Hydrol Earth Syst Sci*, 20, 3601–3618, <https://doi.org/10.5194/hess-20-3601-2016>, 2016.

502 Dang, T. D., Chowdhury, A. K., and Galelli, S.: On the representation of water reservoir storage and operations  
503 in large-scale hydrological models: implications on model parameterization and climate change impact  
504 assessments, *Hydrology and Earth System Sciences Discussions*, 1–34, <https://doi.org/10.5194/hess-2019-334>,  
505 2019.

506 Dang, T. D., Vu, D. T., Chowdhury, A. F. M. K., and Galelli, S.: A software package for the representation and  
507 optimization of water reservoir operations in the VIC hydrologic model, *Environmental Modelling and Software*,  
508 126, 104673, <https://doi.org/10.1016/j.envsoft.2020.104673>, 2020.

509 Dawson, C. W., Abrahart, R. J., and See, L. M.: HydroTest : A web-based toolbox of evaluation metrics for the  
510 standardised assessment of hydrological forecasts, 22, 1034–1052, <https://doi.org/10.1016/j.envsoft.2006.06.008>,  
511 2007.

512 Demargne, J., Wu, L., Regonda, S. K., Brown, J. D., Lee, H., He, M., Seo, D. J., Hartman, R., Herr, H. D.,  
513 Fresch, M., Schaake, J., and Zhu, Y.: The science of NOAA’s operational hydrologic ensemble forecast service,  
514 *Bull Am Meteorol Soc*, 95, 79–98, <https://doi.org/10.1175/BAMS-D-12-00081.1>, 2014.

515 Demeritt, D., Pappenberger, F., Centre, E., Weather, R., and Rg, R.: Challenges in communicating and using  
516 ensembles in operational flood forecasting, 222, 209–222, <https://doi.org/10.1002/met.194>, 2010.

517 Dipti, J.: What is the impact of floods on India’s GDP?,  
518 <https://www.livemint.com/Politics/M1cZ2bfYHSG7yCdHHvUozN/Are-floods-causing-more-damage-these-days.html>, 2017.

520 Dong, N., Wei, J., Yang, M., Yan, D., Yang, C., Gao, H., Arnault, J., Laux, P., Zhang, X., Liu, Y., Niu, J.,  
521 Wang, H., Wang, H., Kunstmann, H., and Yu, Z.: Model Estimates of China’s Terrestrial Water Storage  
522 Variation Due To Reservoir Operation, *Water Resour Res*, 58, <https://doi.org/10.1029/2021WR031787>, 2022.

523 Field, C. B., Barros, V., Stocker, T. F., Dahe, Q., Dokken, D. J., Ebi, K. L., Mastrandrea, M. D., Pauline, K. J.,  
524 Plattner, G.-K., Allen, S. K., Tignor, M., and Midgley, P. M.: Special Report of the Intergovernmental Panel  
525 on Climate Change Edited, 30 pp., 2011.

526 Gain, A. K. and Giupponi, C.: Impact of the Farakka Dam on thresholds of the hydrologic: Flow regime in the  
527 Lower Ganges River Basin (Bangladesh), *Water (Switzerland)*, 6, 2501–2518,  
528 <https://doi.org/10.3390/w6082501>, 2014.

529 Gao, H., Tang, Q., Shi, X., Zhu, C., Bohn, T., and Su, F.: Water Budget Record from Variable Infiltration  
530 Capacity ( VIC ) Model, 120–173 pp., 2009.

531 Georgakakos, A. P., Yao, H., Kistenmacher, M., Georgakakos, K. P., Graham, N. E., Cheng, F. Y., Spencer, C.,  
532 and Shamir, E.: Value of adaptive water resources management in Northern California under climatic variability  
533 and change: Reservoir management, *J Hydrol (Amst)*, 412–413, 34–46,  
534 <https://doi.org/10.1016/j.jhydrol.2011.04.038>, 2012.

535 Gneiting, T. and Raftery, A. E.: Strictly Proper Scoring Rules, Prediction, and Estimation, *J Am Stat Assoc*, 102,  
536 359–378, <https://doi.org/10.1198/016214506000001437>, 2007.

537 Gosain, A. K., Rao, S., and Basuray, D.: Climate change impact assessment on hydrology of Indian river basins,  
538 346–353 pp., 2006.

539 Goswami, S. B., Bal, P. K., and Mitra, A. K.: Use of rainfall forecast from a high-resolution global NWP model  
540 in a hydrological stream flow model over Narmada river basin during monsoon, *Model Earth Syst Environ*, 4,  
541 1029–1040, <https://doi.org/10.1007/s40808-018-0436-y>, 2018.

542 Hagedorn, R., Doblas-Reyes, F. J., and Palmer, T. N.: The rationale behind the success of multi-model  
543 ensembles in seasonal forecasting — I. Basic concept, *Tellus A: Dynamic Meteorology and Oceanography*, 57,  
544 219–233, <https://doi.org/10.3402/tellusa.v57i3.14657>, 2005.

545 Hanasaki, N., Yoshikawa, S., Pokhrel, Y., and Kanae, S.: A global hydrological simulation to specify the sources  
546 of water used by humans, *Hydrol Earth Syst Sci*, 22, 789–817, <https://doi.org/10.5194/hess-22-789-2018>, 2018.

547 Harsha, J.: Fighting floods with insufficient warning, <https://www.thestatesman.com/opinion/fighting-floods-insufficient-warning-1502924062.html>, 2020a.

549 Harsha, J.: Playing catch up in flood forecasting technology, <https://www.thehindu.com/opinion/lead/playing-catch-up-in-flood-forecasting-technology/article32797281.ece>, 2020b.

551 Hersbach, H.: Decomposition of the Continuous Ranked Probability Score for Ensemble Prediction Systems,  
552 2000.

553 Hsiao, L. F., Yang, M. J., Lee, C. S., Kuo, H. C., Shih, D. S., Tsai, C. C., Wang, C. J., Chang, L. Y., Chen, D. Y.  
554 C., Feng, L., Hong, J. S., Fong, C. T., Chen, D. S., Yeh, T. C., Huang, C. Y., Guo, W. D., and Lin, G. F.:  
555 Ensemble forecasting of typhoon rainfall and floods over a mountainous watershed in Taiwan, *J Hydrol (Amst)*,  
556 506, 55–68, <https://doi.org/10.1016/j.jhydrol.2013.08.046>, 2013.

557 Jain, S. K., Mani, P., Jain, S. K., Prakash, P., Vijay, P., Tullos, D., Kumar, S., Agarwal, S. P., and Dimri, A. P.:  
558 A Brief review of flood forecasting techniques and their applications, *Intl. J. River Basin Management*, 0, 1–16,  
559 <https://doi.org/10.1080/15715124.2017.1411920>, 2018.

560 Jarvis, A.: Hole-field seamless SRTM data, International Centre for Tropical Agriculture (CIAT), 2008.

561 Joshi, H.: Floods across the country highlight need for a robust flood management structure,  
562 <https://india.mongabay.com/2020/08/floods-across-the-country-highlight-need-for-a-robust-flood-management-structure/>, 2020.

564 Krzysztofowicz, R.: The case for probabilistic forecasting in hydrology, 249, 2–9,  
565 [https://doi.org/https://doi.org/10.1016/S0022-1694\(01\)00420-6](https://doi.org/https://doi.org/10.1016/S0022-1694(01)00420-6), 2001.

566 Liang, X., Lettenmaier, D. P., Wood, E. F., and Burges, S. J.: A simple hydrologically based model of land  
567 surface water and energy fluxes for general circulation models, *Journal of Geophysical Research: Atmospheres*,  
568 99, 14415–14428, <https://doi.org/10.1029/94JD00483>, 1994.

569 Luo, T., Maddocks, A., Iceland, C., Ward, P., and Winsemius, H.: World's 15 countries with the most people  
570 exposed to river floods., <https://www.wri.org/insights/worlds-15-countries-most-people-exposed-river-floods>,  
571 2015.

572 Madhusoodhanan, C. G., Sreeja, K. G., and Eldho, T. I.: Climate change impact assessments on the water  
573 resources of India under extensive human interventions, *Ambio*, 45, 725–741, <https://doi.org/10.1007/s13280-016-0784-7>, 2016.

575 Meaurio, M., Zabaleta, A., Boithias, L., Epelde, A. M., Sauvage, S., Sánchez-Pérez, J. M., Srinivasan, R., and  
576 Antiguedad, I.: Assessing the hydrological response from an ensemble of CMIP5 climate projections in the  
577 transition zone of the Atlantic region (Bay of Biscay), *J Hydrol (Amst)*, 548, 46–62,  
578 <https://doi.org/10.1016/j.jhydrol.2017.02.029>, 2017.

579 Mediero, L., Garrote, L., and Martín-Carrasco, F.: A probabilistic model to support reservoir operation decisions  
580 during flash floods, *Hydrological Sciences Journal*, 52, 523–537, <https://doi.org/10.1623/hysj.52.3.523>, 2007.

581 Mishra, V., Cherkauer, K. A., Niyogi, D., Lei, M., Pijanowski, B. C., Ray, D. K., Bowling, L. C., and Yang, G.:  
582 A regional scale assessment of land use/land cover and climatic changes on water and energy cycle in the upper  
583 Midwest United States, *International Journal of Climatology*, 30, 2025–2044, <https://doi.org/10.1002/joc.2095>,  
584 2010.

585 Muhammad, A., Stadnyk, T. A., Unduche, F., and Coulibaly, P.: Multi-model approaches for improving  
586 seasonal ensemble streamflow prediction scheme with various statistical post-processing techniques in the  
587 Canadian Prairie Region, *Water (Switzerland)*, 10, <https://doi.org/10.3390/w10111604>, 2018.

588 Mukhopadhyay, P., Krishna, R. P. M., Deshpande, M., Ganai, M., Tirkey, S., Goswami, T., and Sarkar, S.: High  
589 Resolution ( 12 . 5 km ) Ensemble Prediction system based on GEFS : Evaluation of extreme precipitation events  
590 over Indian region, 2–4, 2018.

591 Nanditha, J. S. and Mishra, V.: On the need of ensemble flood forecast in India, *Water Secur*, 12, 100086,  
592 <https://doi.org/10.1016/j.wasec.2021.100086>, 2021.

593 Nanditha, J. S. and Mishra, V.: Multiday Precipitation Is a Prominent Driver of Floods in Indian River Basins,  
594 *Water Resour Res*, 58, e2022WR032723, <https://doi.org/https://doi.org/10.1029/2022WR032723>, 2022.

595 Nash, J. E. and Sutcliffe, J. V.: RIVER FLOW FORECASTING THROUGH CONCEPTUAL MODELS PART  
596 I - A DISCUSSION OF PRINCIPLES\*, *J Hydrol (Amst)*, 10, 282–290, 1970.

597 Pai, D. S., Sridhar, L., Rajeevan, M., Sreejith, O. P., Satbhai, N. S., and Mukhopadhyay, B.: ( 1901-2010 ) daily  
598 gridded rainfall data set over India and its comparison with existing data sets over the region, *Mausam*, 1, 1–18,  
599 2014.

600 Pai, D. S., Sridhar, L., Badwaik, M. R., and Rajeevan, M.: Analysis of the daily rainfall events over India using a  
601 new long period (1901–2010) high resolution ( $0.25^\circ \times 0.25^\circ$ ) gridded rainfall data set, *Clim Dyn*, 45, 755–776,  
602 <https://doi.org/10.1007/s00382-014-2307-1>, 2015.

603 Pappenberger, F., Beven, K. J., Hunter, N. M., Bates, P. D., Gouweleeuw, B. T., Thielen, J., and de Roo, A. P.  
604 J.: Cascading model uncertainty from medium range weather forecasts (10 days) through a rainfall-runoff model  
605 to flood inundation predictions within the European Flood Forecasting System (EFFS), *Hydrol Earth Syst Sci*, 9,  
606 381–393, <https://doi.org/10.5194/hess-9-381-2005>, 2005.

607 Pappenberger, F., Stephens, E., Thielen, J., Salamon, P., Demeritt, D., Jan, S., Wetterhall, F., and Al, L.:  
608 Visualizing probabilistic flood forecast information : expert preferences and perceptions of best practice in  
609 uncertainty communication, <https://doi.org/10.1002/hyp>, 2012.

610 Ramos, M. H., Mathev, T., Thielen, J., and Pappenberger, F.: Communicating uncertainty in hydro-  
611 meteorological forecasts: Mission impossible?, *Meteorological Applications*, 17, 223–235,  
612 <https://doi.org/10.1002/met.202>, 2010.

613 Ray, K., Pandey, P., Pandey, C., Dimri, A. P., and Kishore, K.: On the recent floods in India, *Curr Sci*, 117, 204–  
614 218, <https://doi.org/10.18520/cs/v117/i2/204-218>, 2019.

615 Reed, P. M., Hadka, D., Herman, J. D., Kasprzyk, J. R., and Kollat, J. B.: Evolutionary multiobjective  
616 optimization in water resources: The past, present, and future, *Adv Water Resour*, 51, 438–456,  
617 <https://doi.org/10.1016/j.advwatres.2012.01.005>, 2013.

618 Saleh, F., Ramaswamy, V., Georgas, N., Blumberg, A. F., and Pullen, J.: Inter-comparison between retrospective  
619 ensemble streamflow forecasts using meteorological inputs from ECMWF and NOAA/ESRL in the Hudson  
620 River sub-basins during Hurricane Irene (2011), *Hydrology Research*, 50, 166–186,  
621 <https://doi.org/10.2166/nh.2018.182>, 2019.

622 Shah, R., Sahai, A. K., and Mishra, V.: Short to sub-seasonal hydrologic forecast to manage water and  
623 agricultural resources in India, *Hydrol Earth Syst Sci*, 21, 707–720, <https://doi.org/10.5194/hess-21-707-2017>,  
624 2017.

625 Shah, H. L., Zhou, T., Sun, N., Huang, M., and Mishra, V.: Roles of Irrigation and Reservoir Operations in  
626 Modulating Terrestrial Water and Energy Budgets in the Indian Subcontinental River Basins, *Journal of  
627 Geophysical Research: Atmospheres*, 124, 12915–12936, <https://doi.org/10.1029/2019JD031059>, 2019.

628 Sharma, P. J., Patel, P. L., and Jothiprakash, V.: Impact assessment of Hathnur reservoir on hydrological regimes  
629 of Tapi River, India, *ISH Journal of Hydraulic Engineering*, 27, 433–445,  
630 <https://doi.org/10.1080/09715010.2019.1574616>, 2021.

631 Sheffield, J. and Wood, E. F.: Characteristics of global and regional drought , 1950 – 2000 : Analysis of soil  
632 moisture data from off-line simulation of the terrestrial hydrologic cycle, 112, 1–21,  
633 <https://doi.org/10.1029/2006JD008288>, 2007.

634 Sikder, M. S. and Hossain, F.: Improving operational flood forecasting in monsoon climates with bias-corrected  
635 quantitative forecasting of precipitation, *International Journal of River Basin Management*, 17, 411–421,  
636 <https://doi.org/10.1080/15715124.2018.1476368>, 2019.

637 Singh, O. and Kumar, M.: Flood events , fatalities and damages in India from 1978, 1815–1834,  
638 <https://doi.org/10.1007/s11069-013-0781-0>, 2013.

639 Srivastava, A. K., Rajeevan, M., and Kshirsagar, S. R.: Development of a high resolution daily gridded  
640 temperature data set ( 1969 – 2005 ) for the Indian region, Atmospheric Science Letters, 10, 249–254,  
641 <https://doi.org/10.1002/asl>, 2009.

642 Teja, K. N. and Umamahesh, N. v: Application of Ensemble Techniques for Flood Forecasting in India, Roorkee  
643 Water Conclave, 2020.

644 Tiwari, A. D., Mukhopadhyay, P., and Mishra, V.: Influence of bias correction of meteorological and streamflow  
645 forecast on hydrological prediction in India, J Hydrometeorol, 1–60, <https://doi.org/10.1175/jhm-d-20-0235.1>,  
646 2021.

647 Tiwari, A. D. and Mishra, V.: Sub-Seasonal Prediction of Drought and Streamflow Anomalies for Water  
648 Management in India, Journal of Geophysical Research: Atmospheres, 127, e2021JD035737,  
649 <https://doi.org/https://doi.org/10.1029/2021JD035737>, 2022.

650 Todini, E.: Flood Forecasting and Decision Making in the new Millennium . Where are We ?,  
651 <https://doi.org/10.1007/s11269-017-1693-7>, 2017.

652 Tripathi, P.: Flood Disaster in India : An Analysis of trend and Preparedness Flood Disaster in India : An  
653 Analysis of trend and Preparedness, 2016.

654 Uday Kumar, A. and Jayakumar, K. v.: Hydrological alterations due to anthropogenic activities in Krishna River  
655 Basin, India, Ecol Indic, 108, <https://doi.org/10.1016/j.ecolind.2019.105663>, 2020.

656 Velázquez, J. A., Anctil, F., Ramos, M. H., and Perrin, C.: Can a multi-model approach improve hydrological  
657 ensemble forecasting? A study on 29 French catchments using 16 hydrological model structures, Advances in  
658 Geosciences, 29, 33–42, <https://doi.org/10.5194/adgeo-29-33-2011>, 2011.

659 Wu, W., Emerton, R., Duan, Q., Wood, A. W., Wetterhall, F., and Robertson, D. E.: Ensemble flood  
660 forecasting : Current status and future opportunities, 1–32, <https://doi.org/10.1002/wat2.1432>, 2020.

661 Yassin, F., Razavi, S., Elshamy, M., Davison, B., Saprizia-azuri, G., and Wheater, H.: Representation and  
662 improved parameterization of reservoir operation in hydrological and land-surface models, 3735–3764,  
663 <https://doi.org/https://doi.org/10.5194/hess-23-3735-2019>, 2019.

664 Yun, X., Tang, Q., Wang, J., Liu, X., Zhang, Y., Lu, H., Wang, Y., Zhang, L., and Chen, D.: Impacts of climate  
665 change and reservoir operation on streamflow and flood characteristics in the Lancang-Mekong River Basin, J  
666 Hydrol (Amst), 590, <https://doi.org/10.1016/j.jhydrol.2020.125472>, 2020.

667 Zajac, Z., Revilla-romero, B., Salamon, P., Burek, P., Feyera, A., and Beck, H.: The impact of lake and reservoir  
668 parameterization on global streamflow simulation, J Hydrol (Amst),  
669 <https://doi.org/10.1016/j.jhydrol.2017.03.022>, 2017.

670 Zalachori, I., Ramos, M.-H., Garçon, R., Mathevret, T., and Gailhard, J.: Statistical processing of forecasts for  
671 hydrological ensemble prediction: a comparative study of different bias correction strategies, Advances in  
672 Science and Research, 8, 135–141, <https://doi.org/10.5194/asr-8-135-2012>, 2012.

673 Zarzar, C. M., Hosseiny, H., Siddique, R., Gomez, M., Smith, V., Mejia, A., and Dyer, J.: A Hydraulic  
674 MultiModel Ensemble Framework for Visualizing Flood Inundation Uncertainty, J Am Water Resour Assoc, 54,  
675 807–819, <https://doi.org/10.1111/1752-1688.12656>, 2018.

676 Zhang, J., Chen, J., Li, X., Chen, H., Xie, P., and Li, W.: Combining Postprocessed Ensemble Weather Forecasts  
677 and Multiple Hydrological Models for Ensemble Streamflow Predictions, *J Hydrol Eng*, 25, 04019060,  
678 [https://doi.org/10.1061/\(asce\)he.1943-5584.0001871](https://doi.org/10.1061/(asce)he.1943-5584.0001871), 2020.

679

680